UNCLASSIFIED

AD NUMBER
AD879136
LIMITATION CHANGES

TO:

Approved for public release; distribution is unlimited.

FROM:

Distribution authorized to DoD only; Administrative/Operational Use; JAN 1971. Other requests shall be referred to Air Force Space and Missile Systems Organization, TRD-STINFO, Los Angeles AFB, CA 90045. This document contains export-controlled technical data.

AUTHORITY

samso, usaf ltr, 11 May 1979

THIS PAGE IS UNCLASSIFIED

AEDC-TR-71-3

Copy 1

EXPERIMENTAL INVESTIGATION OF TURBULENT BOUNDARY LAYERS WITH PRESSURE GRADIENT AND HEAT TRANSFER AT MACH NUMBER 4

J. S. Hahn and Ronald G. Lutz

ARO, Inc.

January 1971

VON KÁRMÁN GAS DYNAMICS FACILITY
ARNOLD ENGINEERING DEVELOPMENT CENTER
AIR FORCE SYSTEMS COMMAND
ARNOLD AIR FORCE STATION, TENNESSEE

EXPERIMENTAL INVESTIGATION OF TURBULENT BOUNDARY LAYERS WITH PRESSURE GRADIENT AND HEAT TRANSFER AT MACH NUMBER 4

J. S. Hahn and Ronald G. Lutz

ARO, Inc.

FOREWORD

The work reported herein was done at the request of the Space and Missile Systems Organization (SAMSO), Air Force Systems Command (AFSC), for the Redondo Division of TRW, Inc., under Program Element 63311F, System 627A.

The results presented herein were obtained by ARO, Inc. (a subsidiary of Sverdrup & Parcel and Associates, Inc.), contract operator of the Arnold Engineering Development Center (AEDC), AFSC, Arnold Air Force Station, Tennessee, under Contract F40600-71-C-0002. The tests were conducted during the period from July 13 to August 26, 1970, under ARO Project No. VA0084, and the manuscript was submitted for publication on October 22, 1970.

The tests were conducted under the guidance of Dr. Robert Gran of the Fluid Physics Department of TRW, Inc. The authors wish to acknowledge Richard W. Rhudy of the Supersonic/Hypersonic Branch of the von Kármán Gas Dynamics Facility (VKF) for his assistance during the testing program. The authors also acknowledge Michael B. Krauth and Thomas R. Pyle of the VKF Data Reduction Section for the data reduction programming.

Information in this report is embargoed under the Department of State International Traffic in Arms Regulations. This report may be released to foreign governments by departments or agencies of the U. S. Government subject to approval of SAMSO/TRD-STINFO, or higher authority within the Department of the Air Force. Private individuals or firms require a Department of State export license.

This technical report has been reviewed and is approved.

Emmett A. Niblack, Jr.   Joseph R. Henry
Lt Colonel, USAF   Colonel, USAF
AF Representative, VKF   Director of Test
Directorate of Test

ABSTRACT

An experimental investigation of the behavior of a turbulent boundary layer subjected to adverse and favorable pressure gradients was conducted at Mach number 4 for a free-stream Reynolds number of 0.50×10^6 per inch. Two severe pressure gradients were imposed on the boundary layer by interchangeable, contoured centerbodies inside a large hollow cylinder for cold-wall and adiabatic-wall temperature conditions. Imposition of either of the adverse pressure gradients significantly decreased the natural growth rate of the boundary-layer displacement thickness, whereas the favorable pressure gradient had opposite effects; momentum thickness was relatively unaffected by pressure gradient. A pressure gradient increase of about 30 percent caused relatively small changes in the skin friction, heat-transfer rate, and the characteristic boundary-layer parameters. Wall cooling effects ($T_W/T_O \approx 0.3$) on the boundary-layer thickness parameters were nearly insignificant, in comparison with the adiabatic-wall results. Heat-transfer distributions were similar to the local skin friction results based on free-stream conditions. The behavior of a turbulent, zero-pressure-gradient boundary layer when perturbed by a near-step, wall temperature distribution between two equilibrium states was also investigated. Mach number profiles upstream and well downstream of a step-down in wall temperature were found to be approximately identical. The relaxation of a cold-wall boundary layer toward an adiabatic-wall temperature profile was significantly incomplete far downstream of a step-up in the wall temperature. The data presented include surface pressures, temperatures, skin friction, and heat-transfer rates, as well as boundary-layer Mach number and temperature profiles, and various other boundary-layer properties.

CONTENTS

APPENDIXES

I. ILLUSTRATIONS

Figure

NOMENCLATURE

C_f	Wall skin friction coefficient as measured by a Stanton tube, $288\, \tau_w/(\rho u^2)$
H	Enthalpy, Btu/lb
h	Stanton tube height, in.
M	Mach number
p	Static pressure, psia
q	Dynamic pressure, psia
$\dot{q}$	Heat-transfer rate per unit area, Btu/ft^2-sec
Re_e	Unit Reynolds number per inch outside the boundary layer, $(\rho_e u_e)/(12\,\mu_e)$
Re_∞	Free-stream unit Reynolds number per inch, $(\rho_\infty u_\infty)/(12\,\mu_\infty)$
$Re_{\infty, x}$	Free-stream Reynolds number based on x
St	Stanton number, $\dot{q}/\left[32.174\,\rho_\infty u_\infty\,(H_O - H_W)\right]$
T	Temperature, °R
T_t	Temperature measured by the total-temperature probe, °R
u	Velocity, ft/sec
x	Axial distance downstream from the leading edge of the model wall, in.
y	Distance normal to the model wall, in.
β	Clauser's pressure gradient parameter, $(\delta^*/\tau_w)(dp/dx)_w$

δ	Boundary-layer total thickness ($u/u_e = 0.995$), in.
δ^*	Boundary-layer displacement thickness, in.
θ	Boundary-layer momentum thickness, in.
μ	Absolute viscosity, slugs/ft-sec
ρ	Density, slugs/ft^3
τ_w	Wall shear stress as measured by a Stanton tube, lb/in.^{2}
ϕ	Peripheral angle measured from the main row of static-pressure orifices, positive clockwise when looking upstream, deg (see Fig. 1a)

SUBSCRIPTS

e	Condition outside the boundary layer
o	Tunnel stilling chamber condition
w	Wall condition
∞	Free-stream condition

SECTION I
INTRODUCTION

Predicting the behavior of a compressible turbulent boundary layer, subjected to a pressure gradient and heat transfer, has become the subject of much concern with the advent of large, high-speed, high-altitude vehicles. Although good experimental data are necessary for such predictions, insufficient data presently exist.

The primary objective of the present tests was to obtain complete and reliable experimental skin friction, heat-transfer, and boundary-layer profile (pitot pressure and total temperature) data at two wall temperatures to check the transformation theory proposed by Lewis, Kubota, and Webb (Ref. 1) and future theories for a turbulent boundary layer with arbitrary pressure gradient.

In previous AEDC tests (Ref. 2), the adverse pressure gradient imposed on the boundary layer was linear, giving a variable value of Clauser's pressure gradient parameter (β) which made comparison with the theory difficult. In addition, the earlier tests were conducted only under adiabatic-wall temperature conditions and with a model which had some surface irregularities.

Another objective of the present tests was to study how a turbulent, zero-pressure-gradient boundary layer relaxes between two equilibrium states. The perturbation imposed on the boundary layer was a step (approximately) in the wall temperature distribution.

A large, hollow-cylinder model was selected for the experimental investigation, in an attempt to obtain two-dimensional data (without end effects); a contoured centerbody, designed to produce a constant β value in the adverse pressure gradient region, was used to impose the pressure gradient on the inner-wall boundary layer without centrifugal effects. The tests were conducted under adiabatic-wall, cold-wall, step-up, and step-down wall temperature conditions at Mach number 4 and $Re_\infty/in. = 0.50 \times 10^6$; the boundary-layer was tripped to ensure turbulent flow before pressure gradient application. Model wall measurements included static pressure, Stanton tube pressure, temperature, and heat transfer. Pitot-pressure, static-pressure, and total-temperature probes were used extensively to survey the boundary layer at several model stations.

SECTION II
APPARATUS

2.1 MODEL

The model consisted of a 20.09-in.-diam (inside) hollow cylinder 49.48 in. long and two interchangeable contoured centerbodies which projected 35.52 in. upstream of the hollow cylinder. It is a modified version of the model used in Ref. 2, and its details are shown in Fig. 1, Appendix I.

Modifications to the hollow cylinder included addition of Gardon heat-transfer gages, 11 additional static-pressure orifices in the pressure gradient region, and copper cooling coils to the external periphery. Also, the hollow cylinder was shortened by 0.518 in. during the remachining and handworking of the inside surface. Measurements obtained after the modifications indicated that the variation of the inside radius, over the length of the hollow cylinder, was ±0.005 in., and the surface finish was within 100 μin./in.

Each of the seven sections of copper cooling coils consisted of two spiraled copper tubes (each having an inlet and an outlet). The two spiraled tubes were interwoven such that the flow was in opposite directions in any two adjacent tubes on the surface of the hollow cylinder.

The hollow cylinder was supported by two swept struts which were mounted to the tunnel sidewall. Adjustable vertical struts (Fig. 2), which rested on rubber pads against the top and bottom walls of the tunnel, were used to reduce torsional loading of the strut and support system. The hollow cylinder was aligned in the pitch and yaw planes within ±0.05 deg.

Each of the two new centerbodies (Fig. 1b) formed both adverse and favorable pressure gradient regions inside the hollow cylinder. The contours of the centerbodies were determined from an axisymmetric method of characteristics computer program by TRW personnel. They were designed to produce constant β (Clauser's pressure gradient parameter) values of 4 and 6 in the adverse pressure gradient region, beginning at, approximately, x = 14.5 in.; however, they actually produced β values of 3 and 4 in this region. The centerbodies were cantilevered from a cylindrical hub which was attached to the hollow cylinder near its exit by four support struts as shown in Fig. 1a. By shimming inside the support hub, the centerbodies were aligned in the pitch and yaw planes within ±0.05 deg. An additional centerbody, a short hollow

cylinder, was used for the no-centerbody configuration to eliminate the separated region, observed in previous tests, which was caused by the blunt centerbody support hub.

A 0.375-in.-wide by 0.006-in.-thick piece of fiber glass tape, serrated at the leading edge and located approximately 0.125 in. from the leading edge on the inside surface of the hollow cylinder, was used as a boundary-layer trip for all configurations.

2.2 BOUNDARY-LAYER PROBES AND INSTRUMENTATION

A pitot-pressure probe, a cone-cylinder, static-pressure probe, and a bulb-type, total-temperature probe were employed to survey the boundary layer on the inner wall of the hollow cylinder. The probes (Fig. 1c) were mounted on a cantilevered support arm (Fig. 1d) which could be placed at three different longitudinal positions. The arm was attached to a remotely controlled probe-drive mechanism, which was strut mounted to the tunnel sidewall opposite the model support struts. This combination provided 34.4 in. of longitudinal travel and 2.0 in. of vertical travel from the surface when not restricted by the centerbody.

Initial data, which were obtained using the probe support arm of Ref. 2, indicated that the y-output of the probe-drive mechanism was not identical to the y-location of the probes. The data also indicated that the deflection of the probe-support arm was apparently changing with distance from the model surface. Therefore, a linear, slide-wire potentiometer, attached (11.4 in. downstream of the probes) to a new, more rigid probe-support arm (Fig. 1d), was used to determine vertical probe positioning. Later, another linear, slide-wire potentiometer was installed (6.63 in. downstream of the probes) on the arm to check for possible rotation and to define the deflection at two locations near the probes. The two potentiometers are shown in Fig. 2.

A low-voltage, transistorized fouling circuit was used to establish contact (without an electric arc) between the model wall and the pitot-probe tip or a spike. This spike (attached 0.8 in. from the pitot-probe tip) was used to penetrate any frost that formed on the model wall.

The hollow cylinder portion of the model was instrumented with 77 static-pressure orifices, 38 stanton tubes, 42 Gardon heat-transfer gages, and 8 Chromel® -Alumel® thermocouples. Detailed instrumentation locations are given in Table I (Appendix II).

3

Gardon gage instrumentation (Fig. 1e) consisted of six 0.125-in.-diam gages and thirty-six 0.250-in.-diam gages having disk thicknesses of 0.010 in. and 0.010 in. or 0.20 in., respectively. Each 0.250-in.-diam Gardon gage was instrumented to measure the wall temperature, in addition to the heat-transfer rate.

All model pressure orifice diameters were 0.020 in. (including the Stanton tube orifices, see Fig. 1e). Pitot-probe pressure was measured with a 30-psid transducer, referenced to a near vacuum whenever possible; however, for higher pressures it was sometimes necessary (near the edge of the boundary layer) to use an atmospheric reference pressure, which was measured with a 15-psid transducer. All other pressures were measured with 15-psid transducers, referenced to a near vacuum.

2.3 WIND TUNNEL

Supersonic Wind Tunnel (A) is a continuous, closed-circuit, variable density wind tunnel with an automatically driven, flexible-plate-type nozzle and a 40- by 40-in. test section. The tunnel can be operated at Mach numbers from 1.5 to 6 at maximum stagnation pressures from 29 to 200 psia, respectively, and stagnation temperatures up to 750°R ($M_\infty = 6$). Minimum operating pressures range from about one-tenth to one-twentieth of the maximum at each Mach number. The model may be injected into the tunnel for a test run and then retracted for model cooling or model changes without interrupting the tunnel flow. A description of the tunnel and airflow calibration information may be found in Ref. 3.

SECTION III
PROCEDURES

3.1 TEST CONDITIONS AND TECHNIQUES

A complete list of the wall temperature-centerbody configurations tested is given in Table II. All configurations were tested at the nominal test conditions presented below.

M_∞	p_O, psia	T_O, °R	p_∞, psia	Re_∞/in.
4.0	72	572	0.47	0.50×10^6

In an attempt to duplicate the test conditions for all data points, p_O and T_O were maintained at the values listed above within approximately ±0.5 psia and ±2°R, respectively. Nevertheless, all computations involving pressures and temperatures were made by nondimensionalizing these measurements by p_O and T_O, respectively, which were monitored continuously.

In the reduction of the basic experimental data, it was assumed that the static pressure was constant through the boundary layer and equal to p_w. The total-temperature probe measurements were used to define the total-temperature variation through the boundary layer. The y-position of the probes was computed from the outputs of the two linear potentiometers by allowing for linear arm rotation whenever the two disagreed; when only one linear potentiometer was installed, its output was set equal to y. Wall skin friction results were obtained using the Stanton tube pressure (p_{st}) measurements and the procedures of Ref. 4 which are given below.

$$P^* = \left[\rho_w(p_{st} - p_w)h^2\right]/(\mu_w)^2$$

$$\tau = 0.19952624\,(P^*)^{0.77} \text{ or } \log_{10}(\tau) = 0.77\log_{10}(P^*) - 0.70$$

$$C_{f_\infty} = (288\,\tau_w/\rho_\infty u_\infty^2) = 2\tau(p_\infty/p_w)(T_w/T_\infty)(\mu_w/\mu_\infty)^2/(Re_\infty/\text{in.} \times h)^2$$

The step-up, step-down, and cold-wall temperature distributions were achieved in the following manner. The inlets and outlets of the four upstream sections of cooling coils (x = 2.5 to 23.5 in.) and the aft three sections of cooling coils (x = 23.5 to 38.5 in.) were manifolded together such that LN_2 could be circulated through either the four sections, the three sections, or all seven sections; warm water could be circulated through the remaining sections. Although it was believed that the LN_2 would freeze even hot water in the vicinity of the temperature step (x = 23.5 in.), a significant amount of cold water was required (mixed with the hot water) to attain the near-adiabatic wall temperature desired in the region of water flow.

After attempts to obtain repeatability of the boundary-layer profiles at cold-wall stations were unsuccessful, it was noted that the thickness of the frost layer on the model wall was found to become significant after an appreciable length of time. In order to overcome this difficulty, boundary-layer profiles were only taken during the first 15 to 20 min., once the wall was cooled. Then the model was warmed (for about 15 min.) until the frost disappeared. Finally, the model was cooled (cooling time ≈ 5 min) until the desired temperature distribution was attained again. Although some data were obtained without regard for the frost-layer thickness, the majority of the data were obtained using

5

this frost-elimination procedure. Note that the frost-elimination procedure was not employed for the step-up wall temperature configuration. Cold-wall skin friction data are not shown since the Stanton tubes gave obviously erroneous results. Although the frost-elimination procedure was used in trying to obtain these data, some frost apparently formed on the Stanton tubes.

3.2 DATA PRECISION

The uncertainties for the basic tunnel parameters p_0, T_0, and M_∞ were estimated from repeat calibrations of the p_0 and T_0 instruments and from the repeatability and uniformity of the tunnel flow during calibrations. The parameters p_0, T_0, and M_∞ along with their uncertainties were used to compute the uncertainties in the other parameters dependent on these, assuming a random combination of the uncertainties.

Tunnel Parameter	Uncertainty, percent	Tunnel Parameter	Uncertainty, percent
p_0	±0.4	ρ_∞	±1.1
T_0	±0.2	u_∞	±0.1
M_∞	±0.3	μ_∞	±0.5
p_∞	±1.5	Re_∞	±0.7
q_∞	±1.0	H_0	±0.2
T_∞	±0.5		

The 15-psid and 30-psid transducers have calibrated full-scale ranges of 1, 5, and 15 psia and 2, 10, and 30 psia, respectively. Their precision is considered to be within ±0.3 percent of full scale for the lowest range and ±0.2 percent of full scale for the other ranges.

Estimated precisions in measuring the Stanton tube height, location of the survey probes, and the wall and local temperatures are given below.

Parameter	Uncertainty
h	±0.0005 in.
T_t	±4°R
T_w	±6°R (for $T_w \approx 160°R$)
T_w	±1.5°R (for $T_w \approx 572°R$)
x	±0.010 in.
y	±0.003 in.

Uncertainties are listed below for the model flow field and surface parameters that are presented herein. They were computed by assuming a random combination of the appropriate independent variables using the aforementioned uncertainties and precisions.

Parameter	Uncertainty, percent
C_{f_∞}	±3.8
M_e	±0.4
M/M_e	±0.6
p_w/p_∞	±1.7
$(p_w/p_\infty)/(p_w/p_\infty)_{\phi=0}$	±2.3
Re_e/Re_∞	±1.7
$Re_{\infty,x}$	±0.7
St	±10
T_t/T_O	±0.9
T_w/T_O	±0.4 (at $T_w/T_O \approx 0.92$)
T_w/T_O	±3.8 (at $T_w/T_O \approx 0.3$)

However, the uncertainties in the boundary-layer displacement and momentum thicknesses are presented below in a different form, since they are dependent on δ.

Parameter	Uncertainty
$\delta*/\delta$	±0.008
θ/δ	±0.012

SECTION IV
RESULTS AND DISCUSSION

Surface pressure and temperature distributions along the wall, shown in Figs. 3 and 4, are useful references for analysis of the data presented herein, since the location and severity of both the pressure gradient and temperature gradient regions are illustrated. Values obtained from the fairings shown on these distributions were used in the reduction of the boundary-layer profile data.

The adiabatic-wall and cold-wall pressure data in Fig. 3 agree remarkably well, with the exception of the data for the step-up wall

temperature case which were obtained without using the frost-elimination procedure discussed earlier.

The adiabatic-wall temperature distributions, shown in Fig. 4, were essentially constant and equal to the recovery temperature, as expected. For cold-wall conditions, the adverse pressure gradient caused a wall temperature increase, whereas the favorable pressure gradient had an opposite but less pronounced effect. Although the feasibility of a near-step wall temperature distribution was initially questionable, the success in achieving the near-step-up and near-step-down distributions and the similarity between the two is evident in Fig. 4b.

The circumferential surface pressure distributions at three stations, presented in Fig. 5, were all (including cold-wall data) uniform within ±5 percent of the absolute static pressure.

The local skin friction coefficient variation along the model wall is shown in Fig. 6. The skin friction data were obtained from Stanton tube and wall static-pressure measurements using the procedures given in Section 3.1. The results presented in Fig. 6a are based on free-stream conditions since complete boundary-layer surveys were not taken for all configurations. Skin friction data based on the local conditions outside the boundary layer and on the data fairings in Fig. 6a are shown in Fig. 6b. Comparisons of the data in Fig. 6a with the laminar theory of Cohen and Reshotko (Ref. 5) and the turbulent theory of van Driest (Refs. 6 and 7) are reasonably consistent. The zero-pressure-gradient data were somewhat scattered and generally were about 20 percent lower than van Driest's theory. The results in Fig. 6a show that the skin friction distributions based on free-stream conditions were similar to the wall pressure distributions in imposed pressure gradient regions; however, skin friction coefficient based on local conditions (Fig. 6b) was nearly constant over a portion of the adverse region and significantly increased over part of the favorable pressure gradient region because of the local dynamic pressure variation. With the exception of two points obtained for centerbody A near the peak in the pressure distribution ($18 < x < 20$ in.), the locally based skin friction was not significantly changed by a 30 percent increase in the pressure gradient.

The Gardon gage heat-transfer data presented in Fig. 7 have trends similar to the free-stream skin friction data. These data are noted to be in substantial agreement with the turbulent theory of Ref. 8 just before the pressure rise. As would be expected from the preceding discussion, the spread in the heat-transfer rates would be reduced significantly if the Stanton numbers were based on local conditions.

The variations of the local flow conditions and the boundary-layer thickness parameters are presented in Figs. 8 and 9 for adiabatic- and cold-wall conditions. The effects of an adverse pressure gradient were to decrease the Mach number, increase the Reynolds number, and significantly decrease the natural growth rate of the boundary-layer displacement thickness, whereas a favorable pressure gradient had opposite effects. When the wall was cooled, the boundary-layer displacement thickness was decreased slightly, whereas the momentum thickness was still generally unaffected. These same effects were observed in the cold-wall region for the step-down wall temperature configuration.

Summary Mach number and total temperature profiles are shown in Figs. 10 and 11, respectively. The effect of cooling the wall, shown in Fig. 10, was to make the Mach number profiles fuller than the adiabatic-wall profiles. The temperature profile results given in Fig. 11 were obtained by interpolating the total-temperature probe data to coincide with the pitot probe heights, and in addition, were extrapolated to the wall using the faired T_W/T_O values from Fig. 4. The actual measurements were made no closer to the wall than about 0.040 in. The relaxation of a cold-wall temperature profile toward an adiabatic-wall profile (shown in Fig. 11d) was a relatively slow process, since the profile was still significantly different from an adiabatic-wall profile at x = 33.5 in., 10 in. downstream of the step-up in wall temperature.

Mach number profiles of boundary layers with imposed adverse and favorable pressure gradients are compared in Fig. 12 under adiabatic-wall and cold-wall temperature conditions. In each instance a turbulent, zero-pressure gradient profile (x = 11.5 in.) is presented for reference. Although this profile was obtained with centerbody B installed, it should be identical to a profile at the same station for centerbody A (see pressure gradient curves in Fig. 3). Under adiabatic-wall temperature conditions (Fig. 12a), an adverse pressure gradient made the Mach number profile less full than the zero-pressure-gradient profile, whereas it was made fuller in a favorable pressure gradient region. However, the cold-wall data with centerbody B, presented in Fig. 12b, apparently did not follow this trend. This suggests that a small height discrepancy may still exist in these cold-wall data despite the precautions taken to minimize the effects of frost formation.

Mach number profiles in the vicinity of and several inches downstream of the step-down in wall temperature (x ≈ 23.5 in.) are shown in Fig. 13. These results show that the Mach number profile remained essentially unchanged at stations from 2 in. upstream of the step to 8 in. (x = 31.5 in.) downstream of the step.

SECTION V
CONCLUDING REMARKS

The influence of pressure gradients imposed on the turbulent boundary layer of a large, hollow cylinder under adiabatic-wall and cold-wall temperature conditions, and the influence of an approximate step in the wall temperature under zero-pressure-gradient conditions were investigated at Mach number 4 for $Re_\infty/in. = 0.50 \times 10^6$. Data obtained included boundary-layer pitot pressure and total temperature, in addition to model surface pressures, temperatures, heat-transfer rates, and Stanton tube pressures. The following statements are a summary of the significant results and conclusions obtained from these data.

1. Imposing a severe adverse pressure gradient $\left[(\delta^*/\tau_w)(dp/dx)_w \approx 3 \text{ or } 4\right]$ on a turbulent boundary layer under adiabatic-wall and cold-wall conditions decreased the natural growth rate of the boundary-layer displacement thickness, decreased the local Mach number, and increased the local Reynolds number; imposing a favorable pressure gradient of similar magnitude had opposite effects. However, momentum thickness was relatively unaffected by either pressure gradient.

2. Stanton tube skin friction coefficient (based on local conditions) generally increased in the adverse pressure gradient region and over a portion of the favorable pressure gradient region.

3. Increasing the pressure gradient by about 30 percent caused relatively small changes in the skin friction, heat-transfer rate, boundary-layer thickness parameters, local flow conditions, and adiabatic-wall Mach number profiles.

4. Effects of wall cooling on the aforementioned thickness parameters and local conditions were almost insignificant, in comparison with the adiabatic-wall results. Nevertheless, cold-wall boundary-layer displacement thickness values were generally somewhat smaller than the adiabatic-wall values.

5. The heat-transfer distributions had trends similar to the local skin friction results based on free-stream conditions.
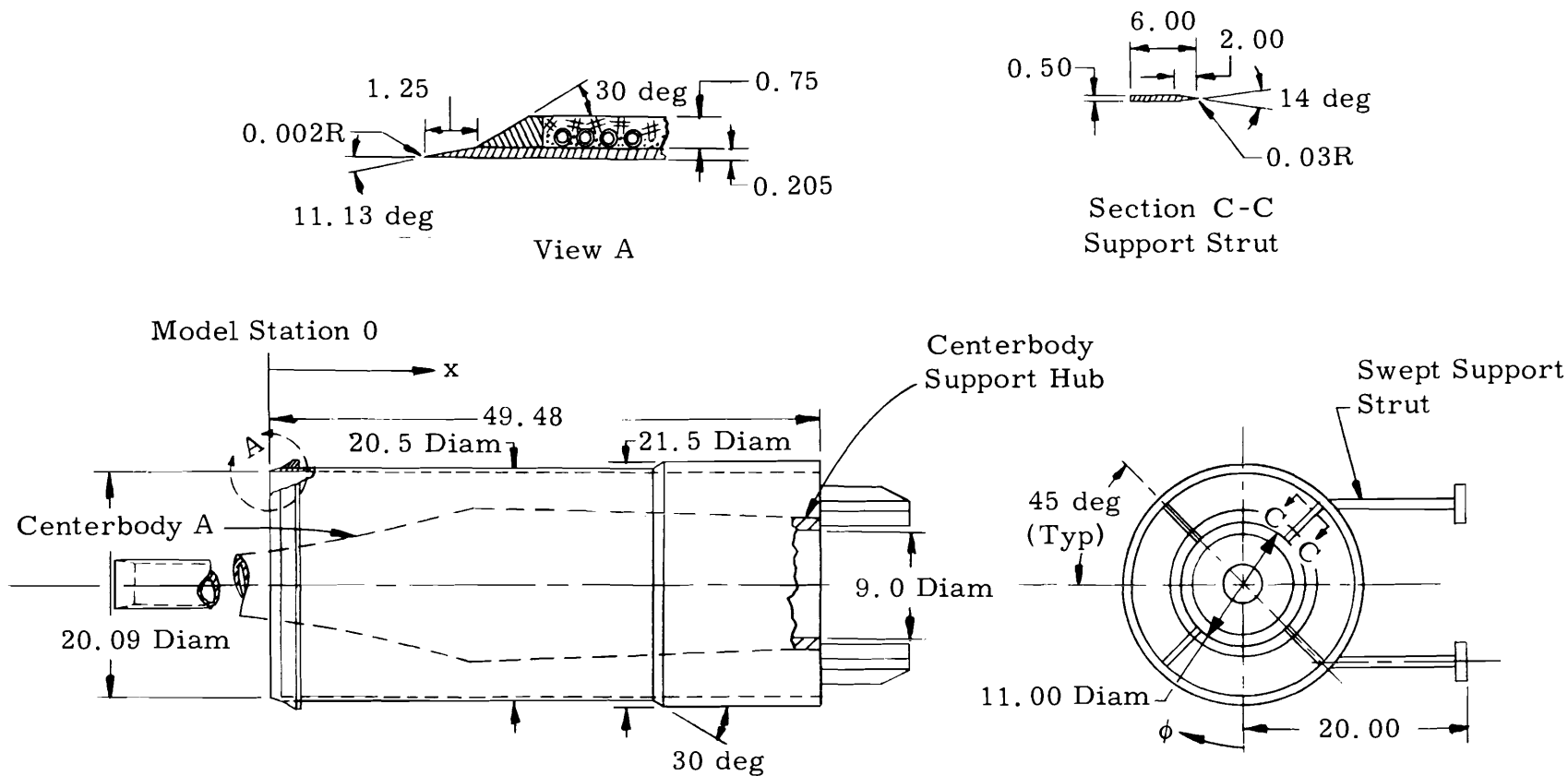
6. Mach number profiles upstream and well downstream of a step-down in wall temperature were approximately identical. In addition, conclusion (4) generally applies to the cold-wall region of the step-down temperature distribution.

7. The relaxation of a cold-wall, turbulent boundary layer toward an adiabatic-wall temperature profile was significantly incomplete far downstream of a step-up in the wall temperature.

REFERENCES

1. Lewis, J. E., Kubota, T., and Webb, W. H. "Transformation Theory for the Compressible Turbulent Boundary Layer with Arbitrary Pressure Gradient." AIAA Paper No. 69-160, Presented at AIAA 7th Aerospace Sciences Meeting, New York, N. Y., January 20-22, 1969.

2. Hahn, Jerry S. "Experimental Investigation of Adiabatic-Wall Turbulent Boundary Layers with Pressure Gradient at Mach Number 4." AEDC-TR-70-31 (AD866883L), April 1970.

3. Test Facilities Handbook (Eighth Edition). "Von Kármán Gas Dynamics Facility, Vol. 4." Arnold Engineering Development Center, December 1969 (AD863646).

4. Smith, K. G., Gaudet, L., and Winter, K. G. "The Use of Surface Pitot Tubes as Skin-Friction Meters at Supersonic Speeds." R & M No. 3351, June 1962.

5. Cohen, C. B. and Reshotko, E. "Similar Solutions for the Compressible Laminar Boundary Layer with Heat Transfer and Pressure Gradient." NACA TN 3325, February 1955.

6. Van Driest, E. R. "The Problem of Aerodynamic Heating." Aeronautical Engineering Review, Vol. 15, No. 10, October 1956, pp. 26-41.

7. Van Driest, E. R. "The Turbulent Boundary Layer with Variable Prandtl Number." North American Aviation, Inc., Report No. AL-1914 (AD49814), April 1954.

8. Harms, R. J., Schmidt, C. M., Hanawalt, A. J., and Schmitt, D. A. "A Manual for Determining Aerodynamic Heating of High-Speed Aircraft." Bell Aircraft Corporation, Report No. 7006-3352-001 (AD229434), June 1959.
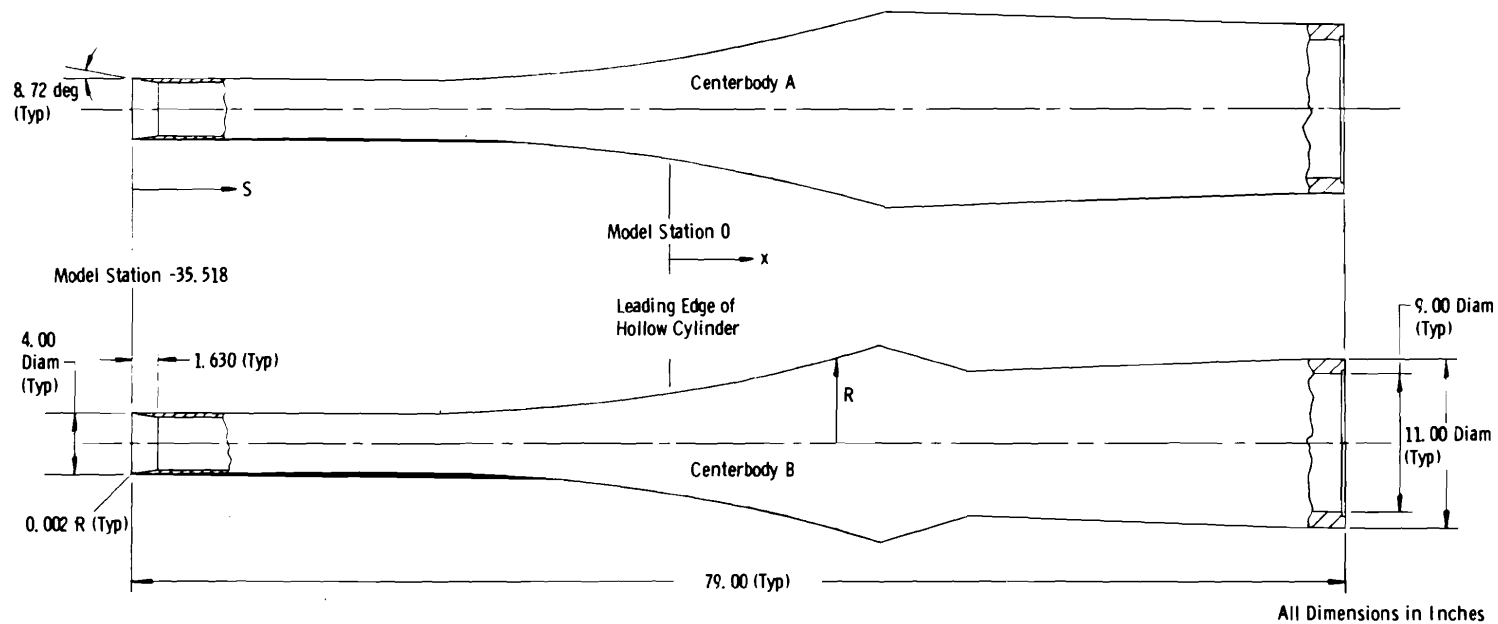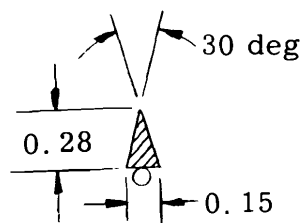
APPENDIXES

I. ILLUSTRATIONS
II. TABLES

View A

Section C-C
Support Strut

30 deg

0.75

1.25

0.002R

11.13 deg

0.205

6.00

2.00

0.50

14 deg

0.03R

Model Station 0

x

Centerbody
Support Hub

Swept Support
Strut

49.48

20.5 Diam

21.5 Diam

A

Centerbody A

45 deg
(Typ)

9.0 Diam

20.09 Diam

11.00 Diam

φ

20.00

30 deg

All Dimensions in Inches

a. Hollow Cylinder
Fig. 1 Details of Model and Boundary-Layer Probes

Centerbody A (β · 4)				Centerbody B (β · 6)			
S	R	S	R	S	R	S	R
0	2.000*	40.38	4.173	0	2.000*	43.36	4.927
16.00	1.910*	41.56	4.423	19.00	1.893*	44.25	5.154
19.00	1.893	42.66	4.665	22.39	2.005	45.08	5.374
22.29	2.000	43.68	4.903	28.34	2.425	45.86	5.587
25.28	2.188	44.63	5.134	32.74	2.925	46.58	5.796
27.96	2.384	45.52	5.360	34.50	3.175	47.27	5.999
30.35	2.616	46.36	5.580	36.07	3.426	47.92	6.196
32.48	2.869	47.15	5.796	37.52	3.680	48.53	6.388
34.39	3.130	47.90	6.006	38.88	3.936	48.55	6.395*
36.11	3.395	48.61	6.214	40.15	4.193	54.58	4.675*
37.67	3.659	49.23	6.380*	41.32	4.446	76.00	5.500*
39.08	3.919	76.00	5.500*	42.38	4.690	79.00	5.500*
		79.00	5.500*				

*Model contour is straight line between consecutive points.

b. Centerbodies
Fig. 1 Continued

30 deg

0.28

0.15

Section D-D (Typ)

0.083

0.018

0.009

Pitot Probe Tip

0.25

2.37

30 deg

D

1.25

0.60

D

6 deg

0.063 OD

0.093 OD
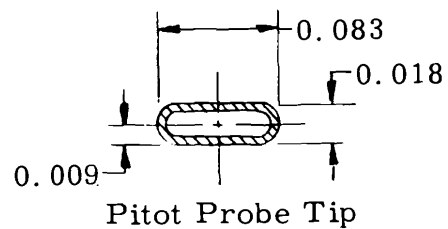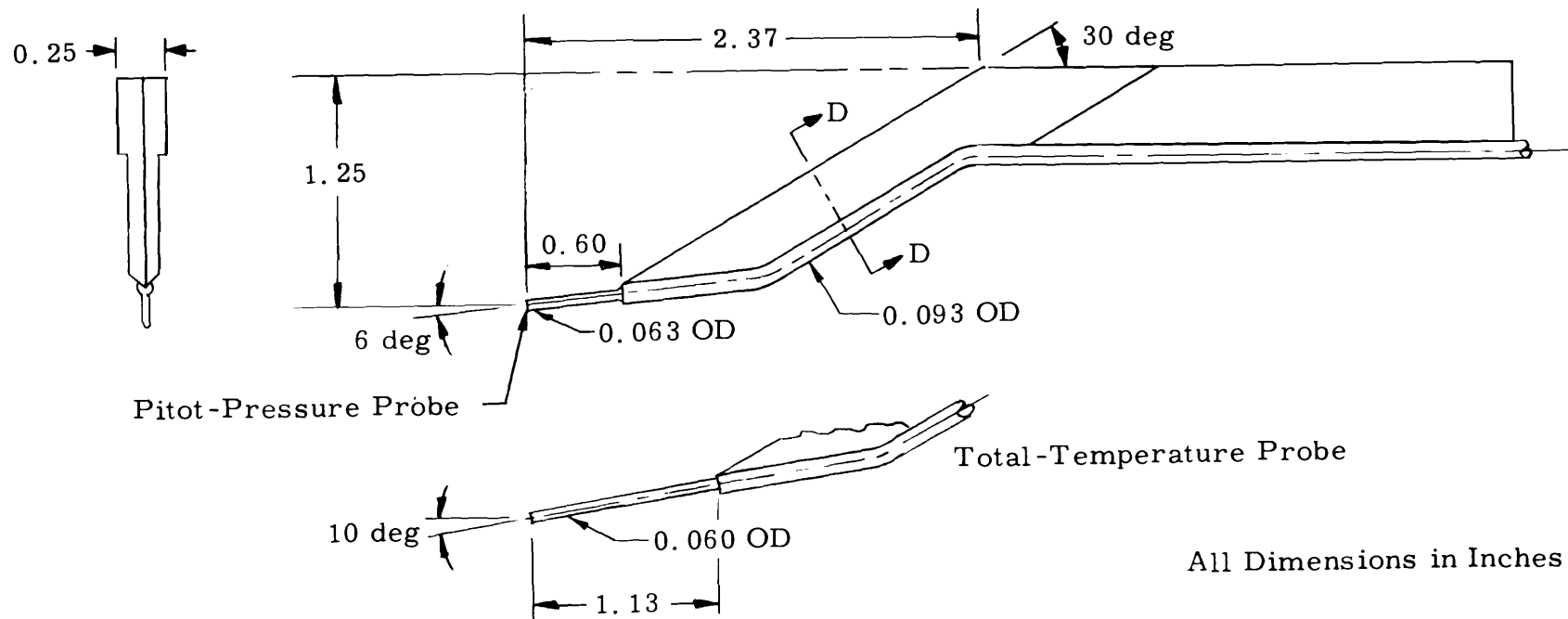
Pitot-Pressure Probe

Total-Temperature Probe

10 deg

0.060 OD

All Dimensions in Inches

1.13

c. Boundary-Layer Probes
Fig. 1 Continued

0.26

1.19

2.75

1.00

0.37

3.33

0.50

0.725

0.875

2.50

30 deg

1.25

0.50

5.00

2.75

22.04

3.43

59.91

Total Temperature Probe

Pitot-Pressure Probe

Static-Pressure Probe (Data Not Presented)

All Dimensions in Inches
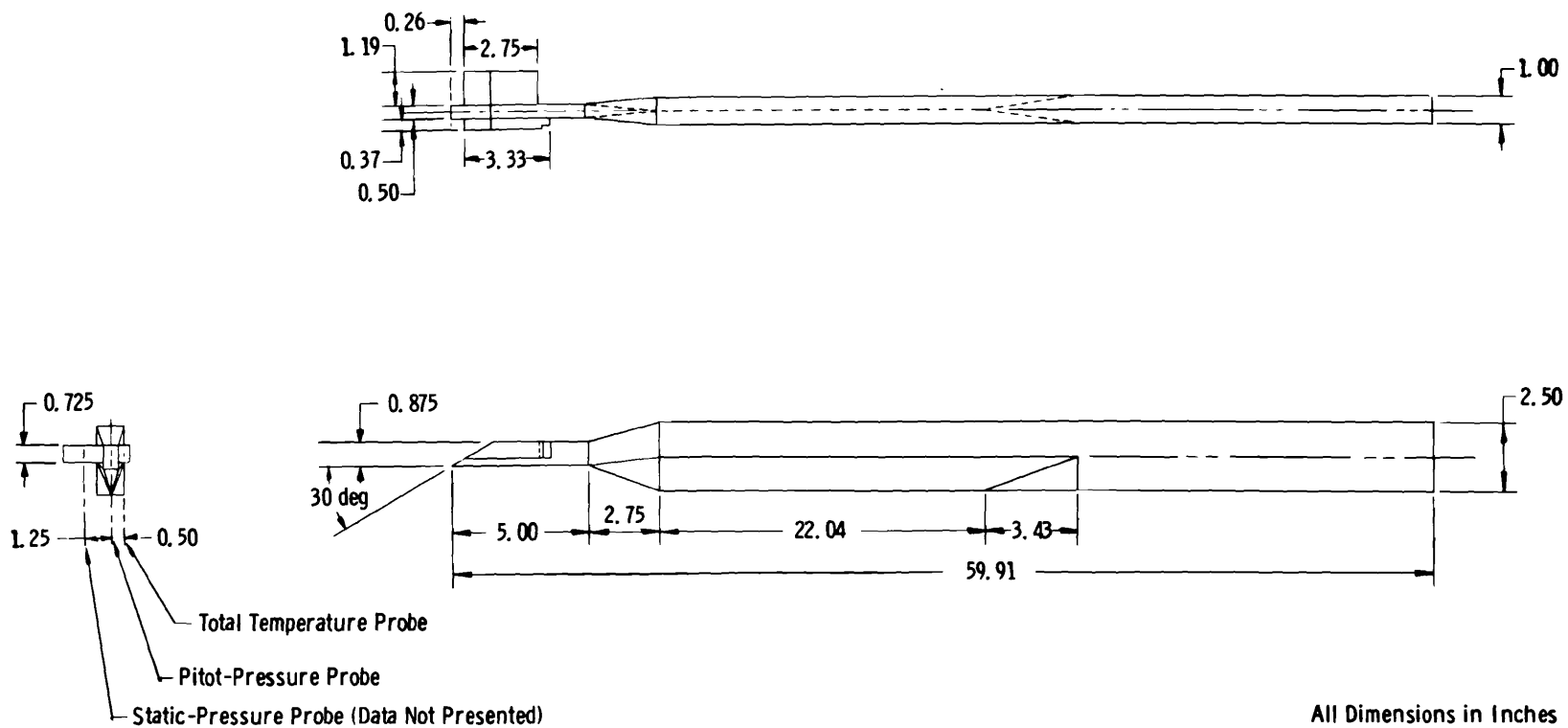
d. Support Arm for Boundary-Layer Probes
Fig. 1 Continued

Capacitance Weld
Inside Surface

0.030

0.250 Diam

Chromel-Alumel
Thermocouple
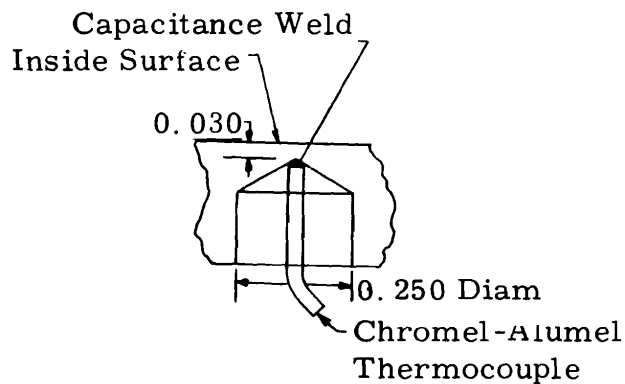
Typical Thermocouple
Installation

Capacitance Weld

0.190

0.095

0.190

Sealed around Three
Sides with Epoxy

6.00 deg

0.015 to 0.025

Inside Surface

h
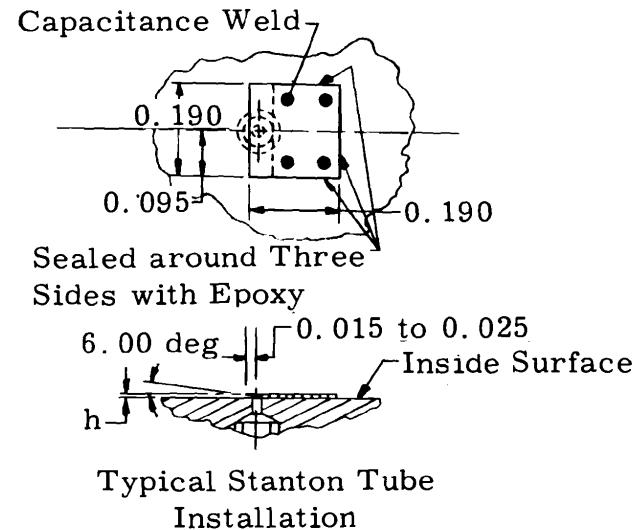
Typical Stanton Tube
Installation

All Dimensions in Inches

0.50

₵

0.375 OD Copper Tubing
Soft-Soldered to Model Wall

Insulating Material Held in
Place with Fiber Glass Tape

0.20

Model Wall

Inside Surface

0.250 Diam (or 0.125 Diam)
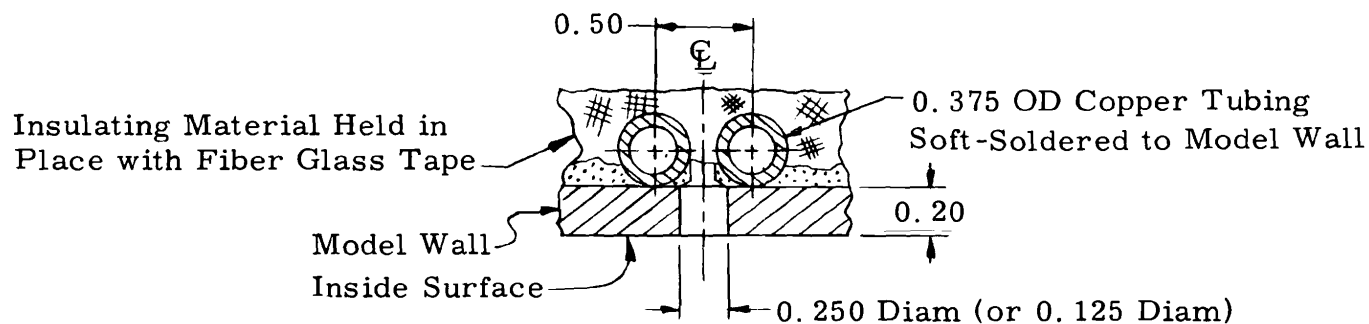
Typical Gardon Gage
Installation

e. Instrumentation
Fig. 1 Concluded
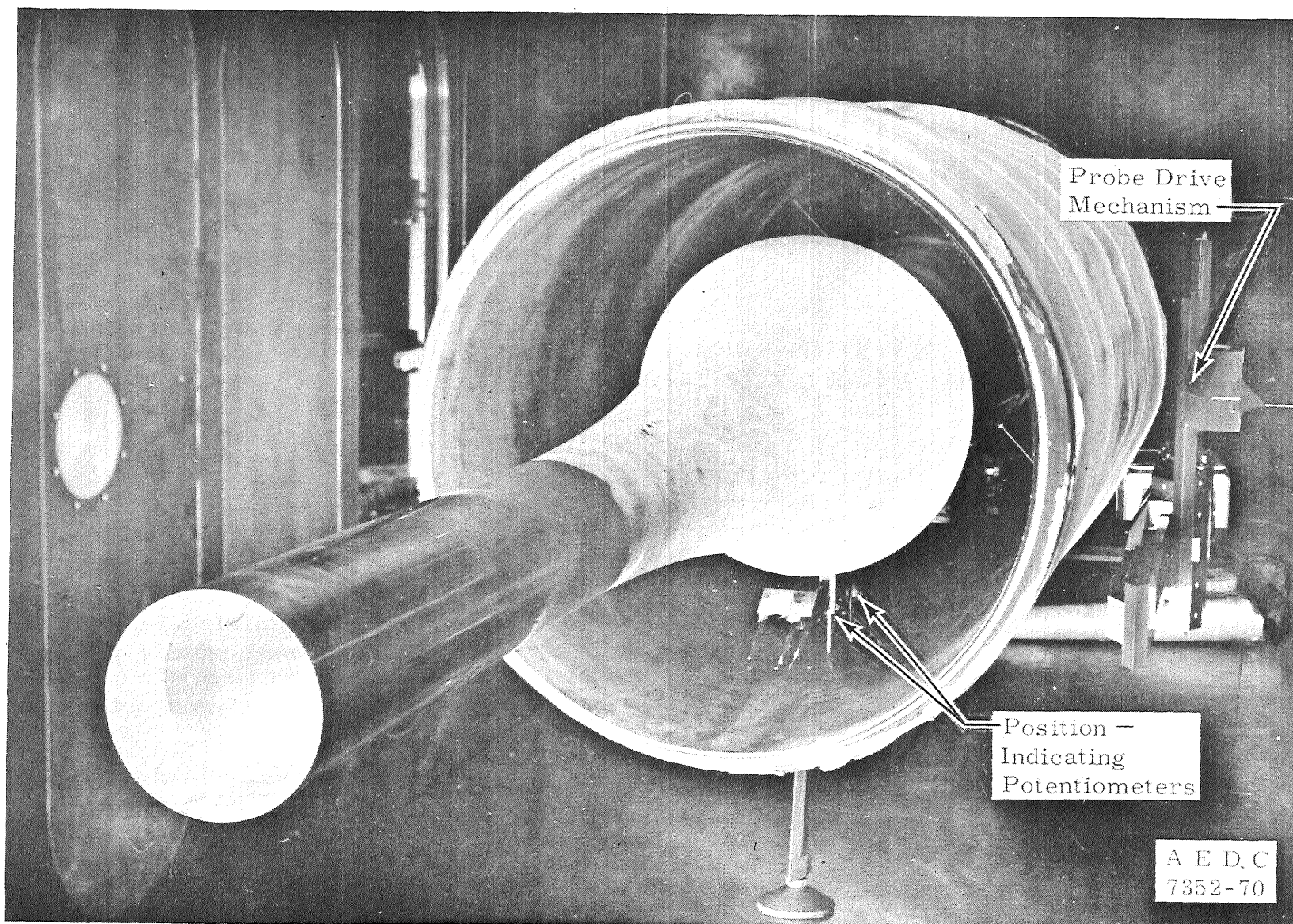
Fig. 2 Model Installation Photograph (Centerbody B)
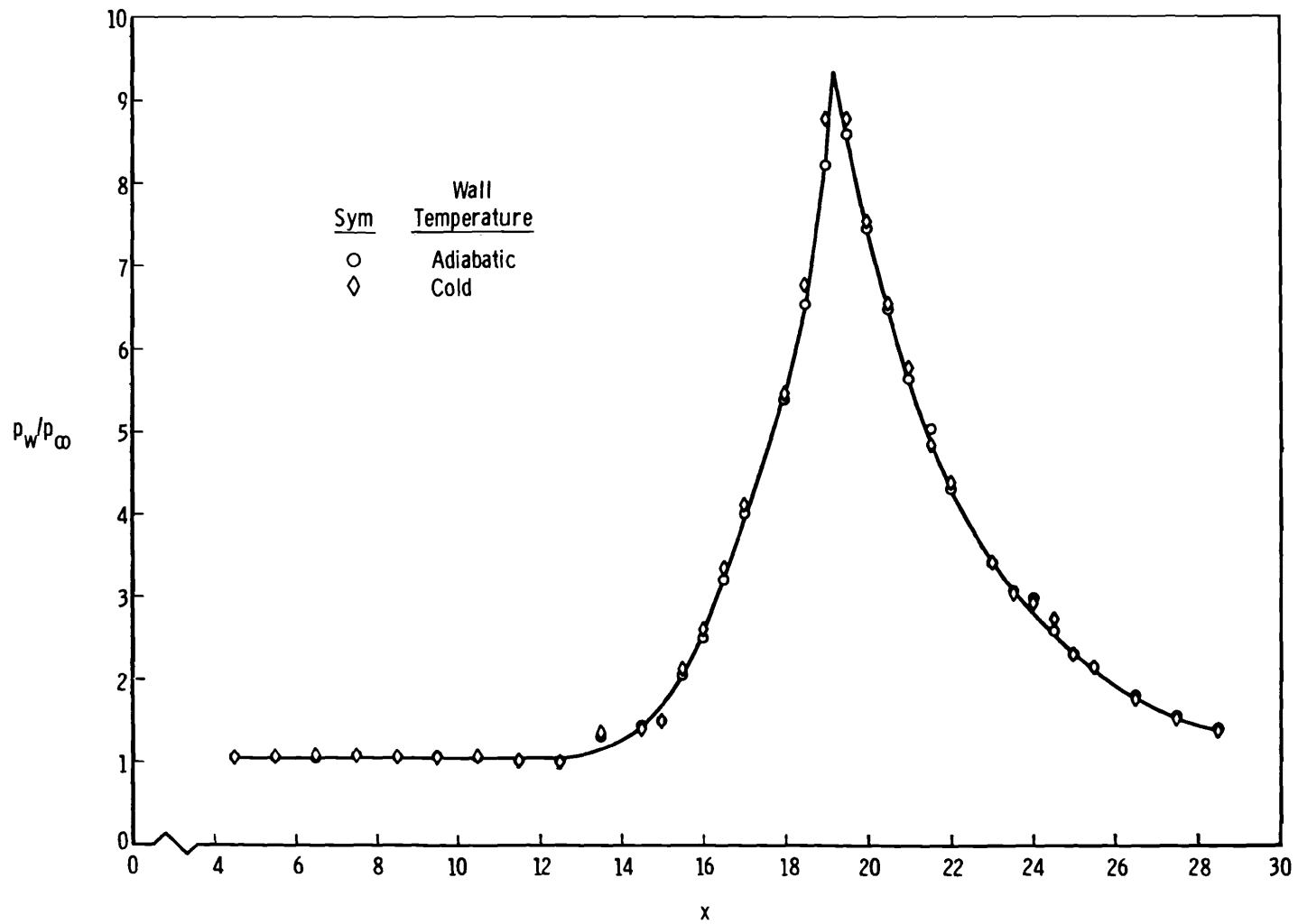
a. Centerbody A ($\beta = 4$)

Fig. 3 Longitudinal Wall Pressure Distributions
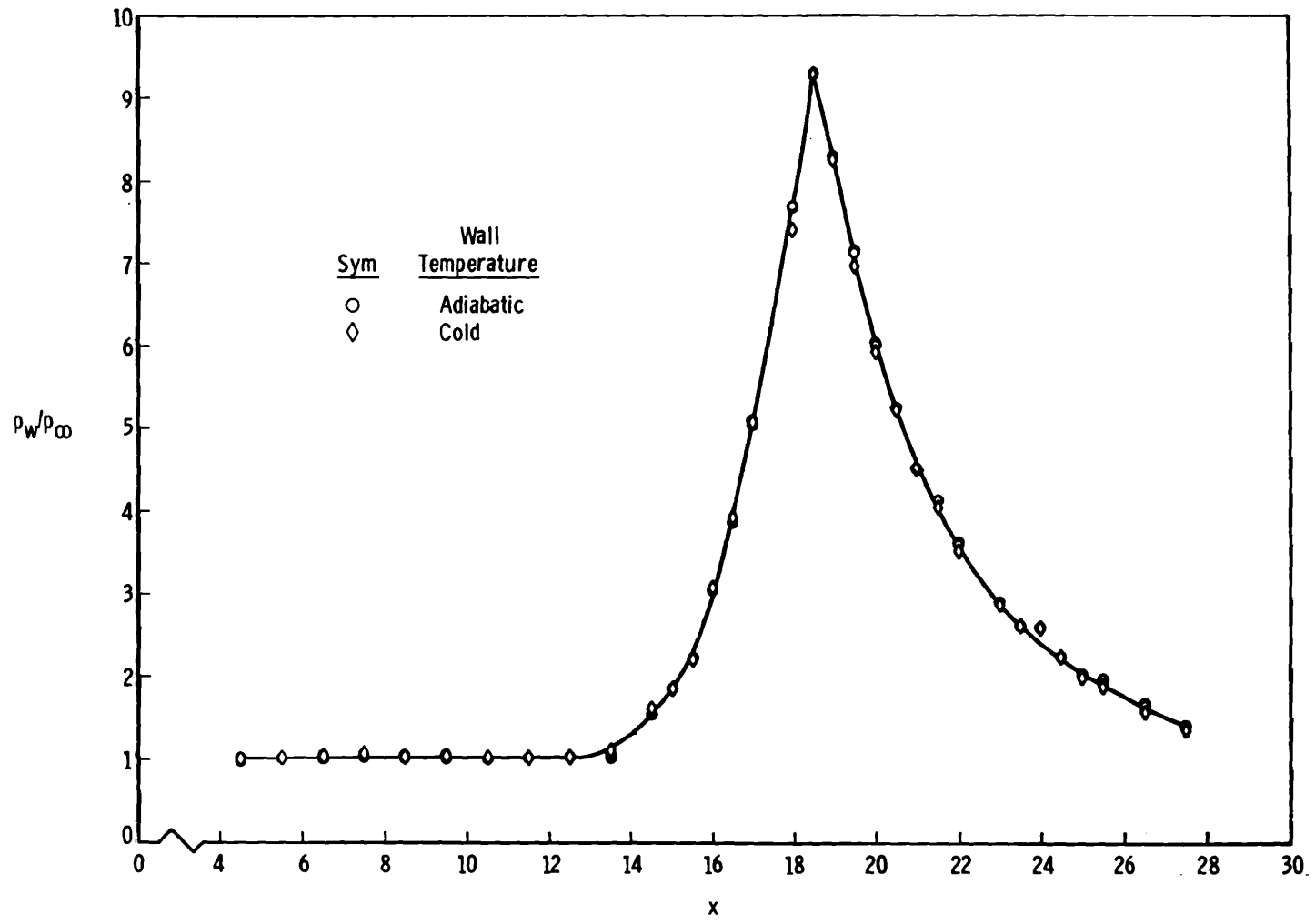
b. Centerbody B (β = 6)
Fig. 3 Continued
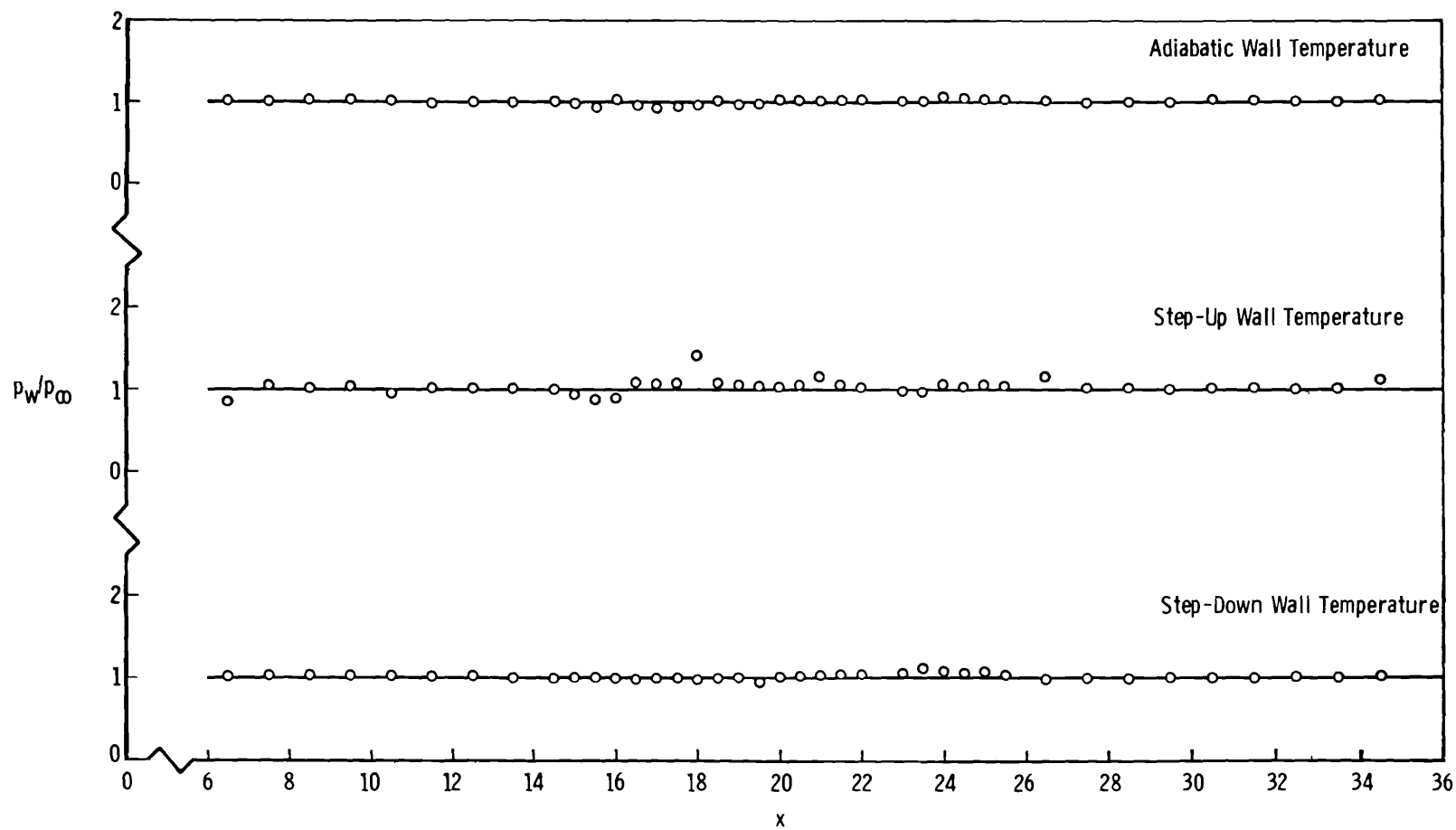
c. No Centerbody
Fig. 3 Concluded

Open Symbols Denote that the Temperature was Measured with a Gardon Gage
Closed Symbols Denote that the Temperature was Measured with a Chromel-Alumel Thermocouple
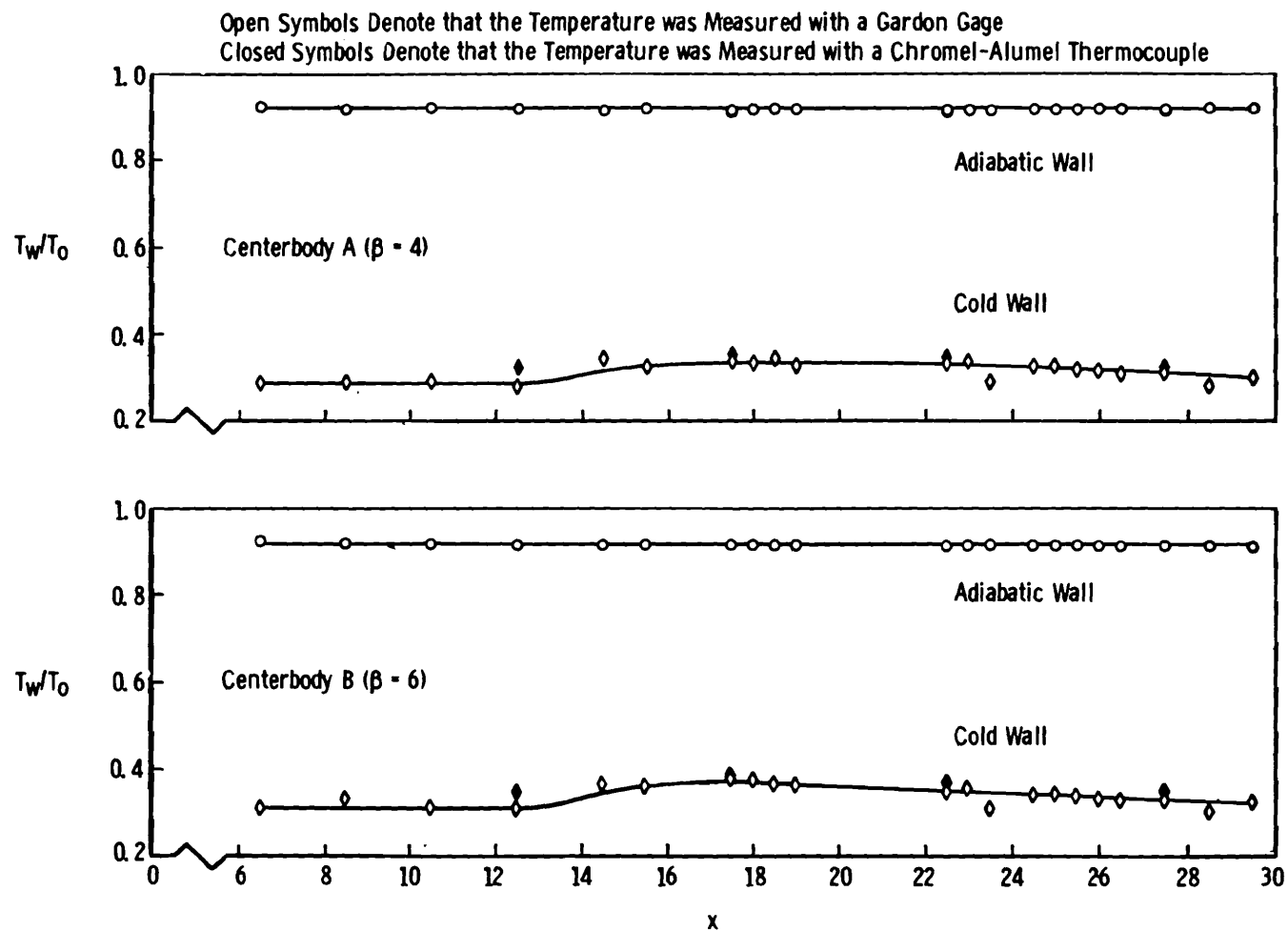
a. Centerbodies A and B
Fig. 4 Model Wall Temperature Distributions

Open Symbols Denote that the Temperature was Measured with a Gardon Gage
Closed Symbols Denote that the Temperature was Measured with a Chromel-Alumel Thermocouple
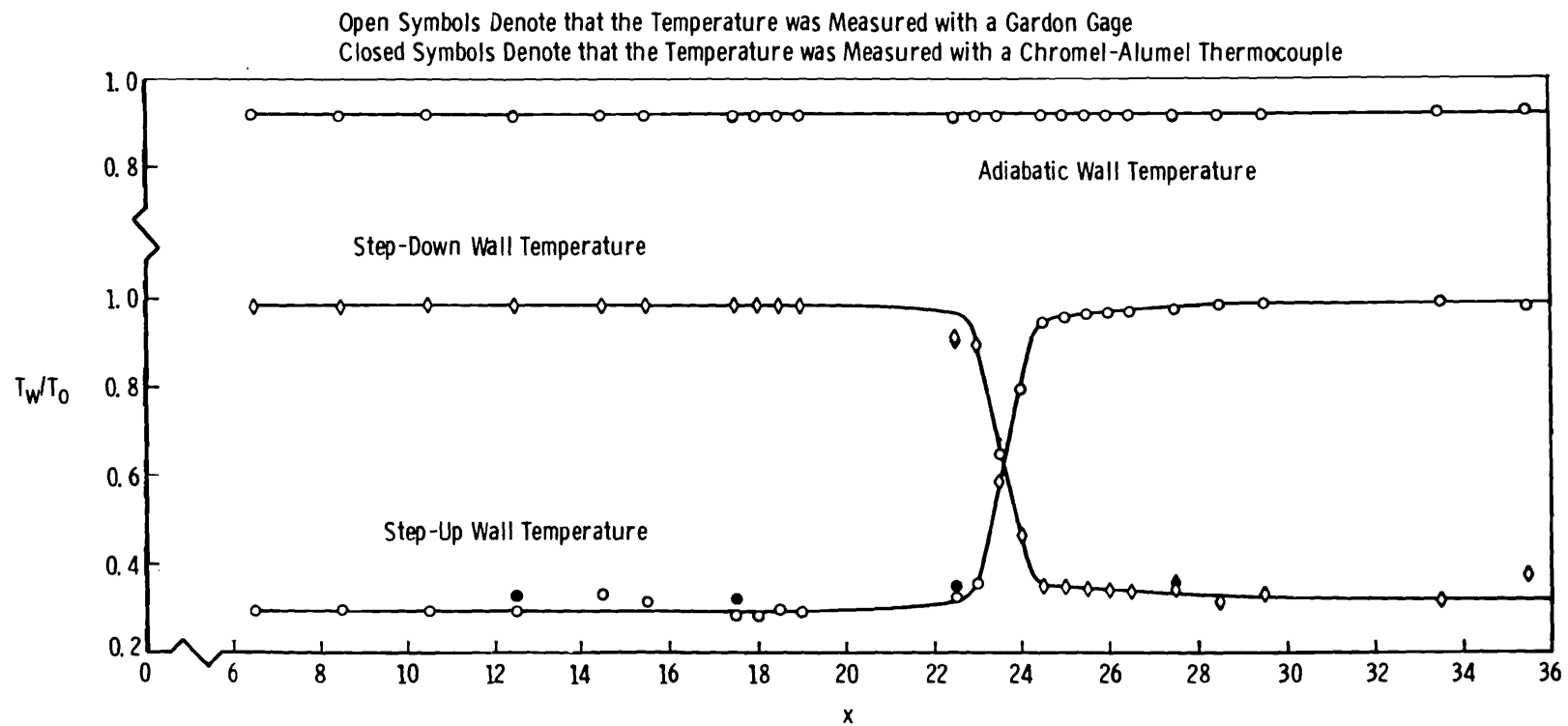
b. No Centerbody
Fig. 4 Concluded

Sym	x, in.	Wall Temperature
◯	2.5	Adiabatic
◻	17.5	Adiabatic
◇	26.5	Adiabatic

No Centerbody

Centerbody A

Centerbody B

ϕ, deg
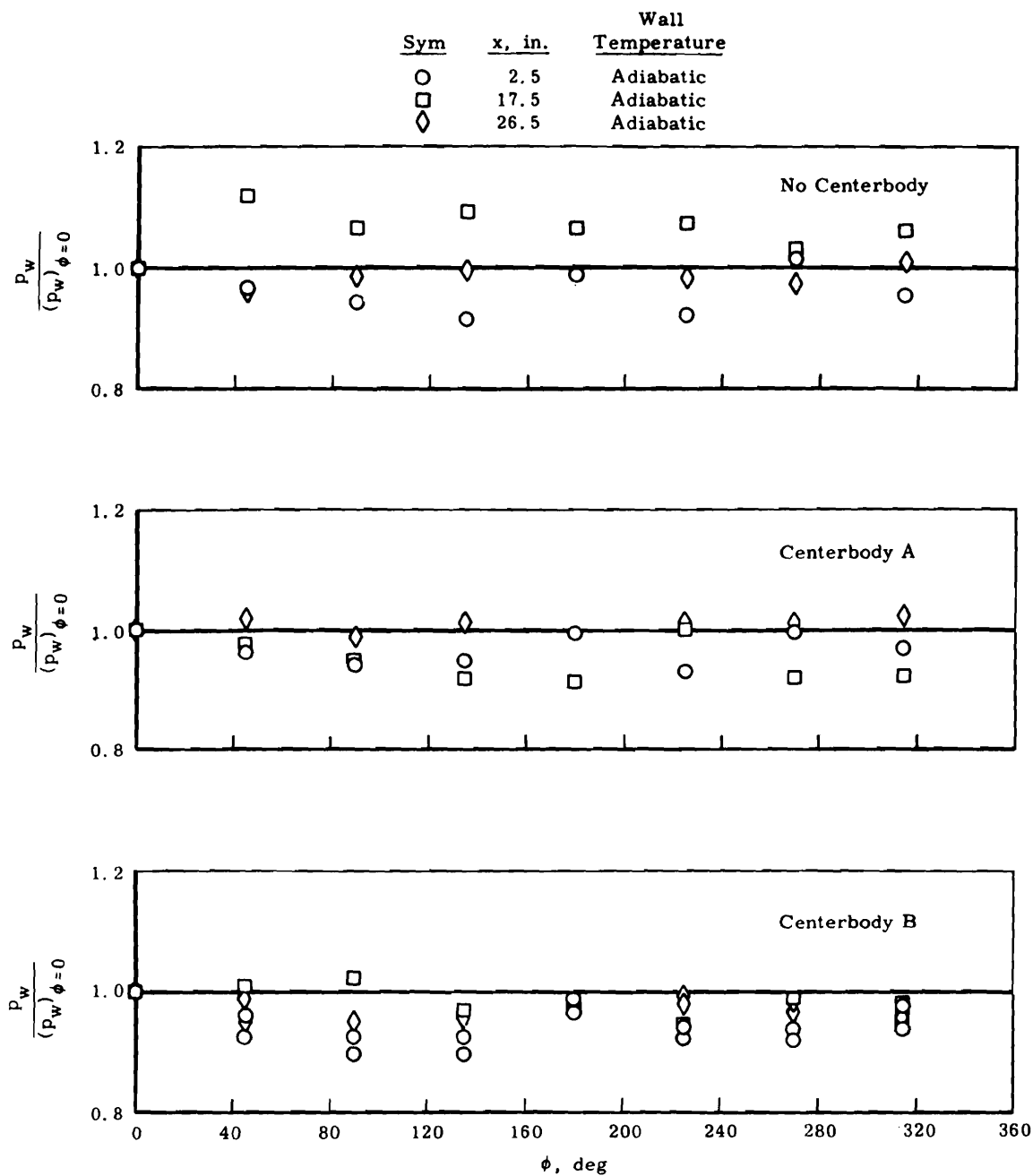
Fig. 5 Circumferential Wall Pressure Distributions at Three Stations for Each Centerbody Configuration
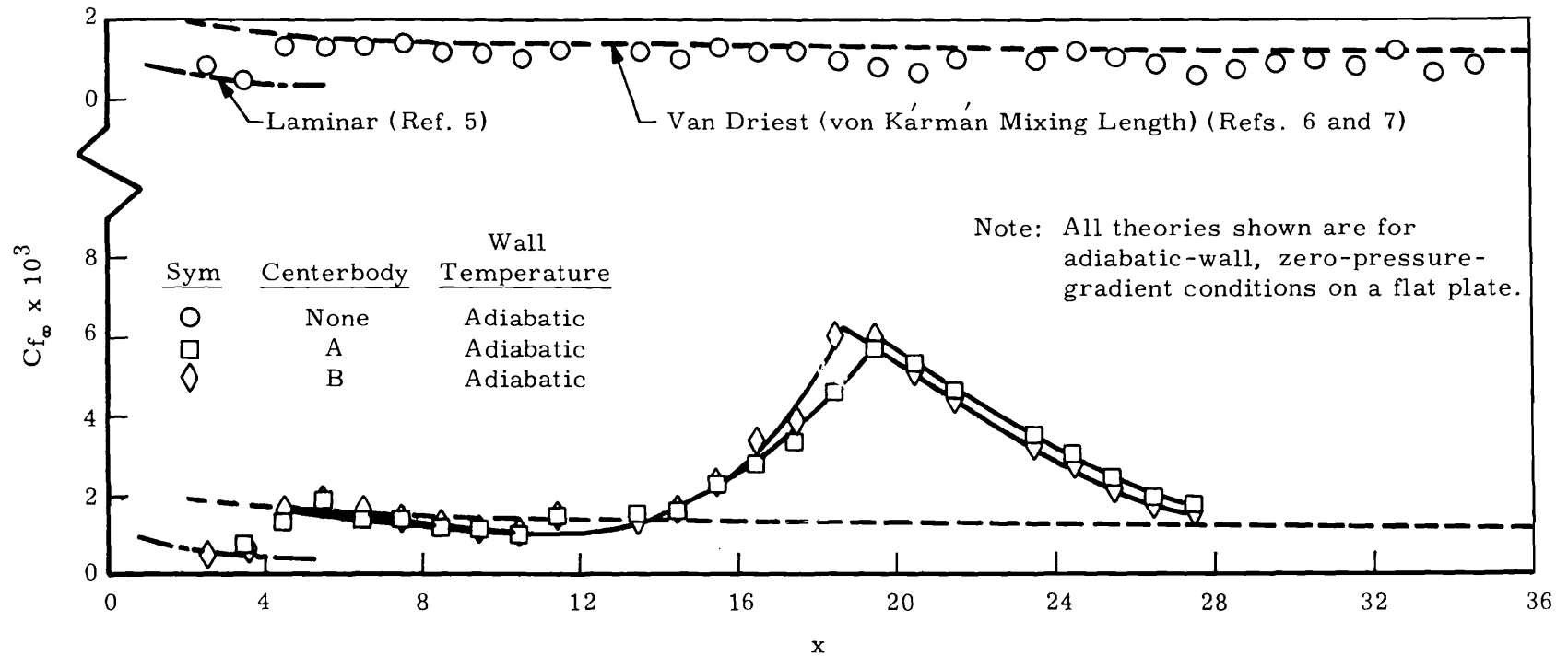
a. Based on Free-Stream Conditions
Fig. 6 Local Skin Friction Coefficient

Sym	Centerbody	Wall Temperature
O	None	Adiabatic
□	A	Adiabatic
◊	B	Adiabatic

Note: The theory shown is for adiabatic-wall, zero-pressure-gradient conditions on a flat plate.

Note: These data were computed based on the data fairings of Fig. 6a.

Van Driest (von Kármán Mixing Length) (Refs. 6 and 7)

$C_{f_e} \times 10^3$

x
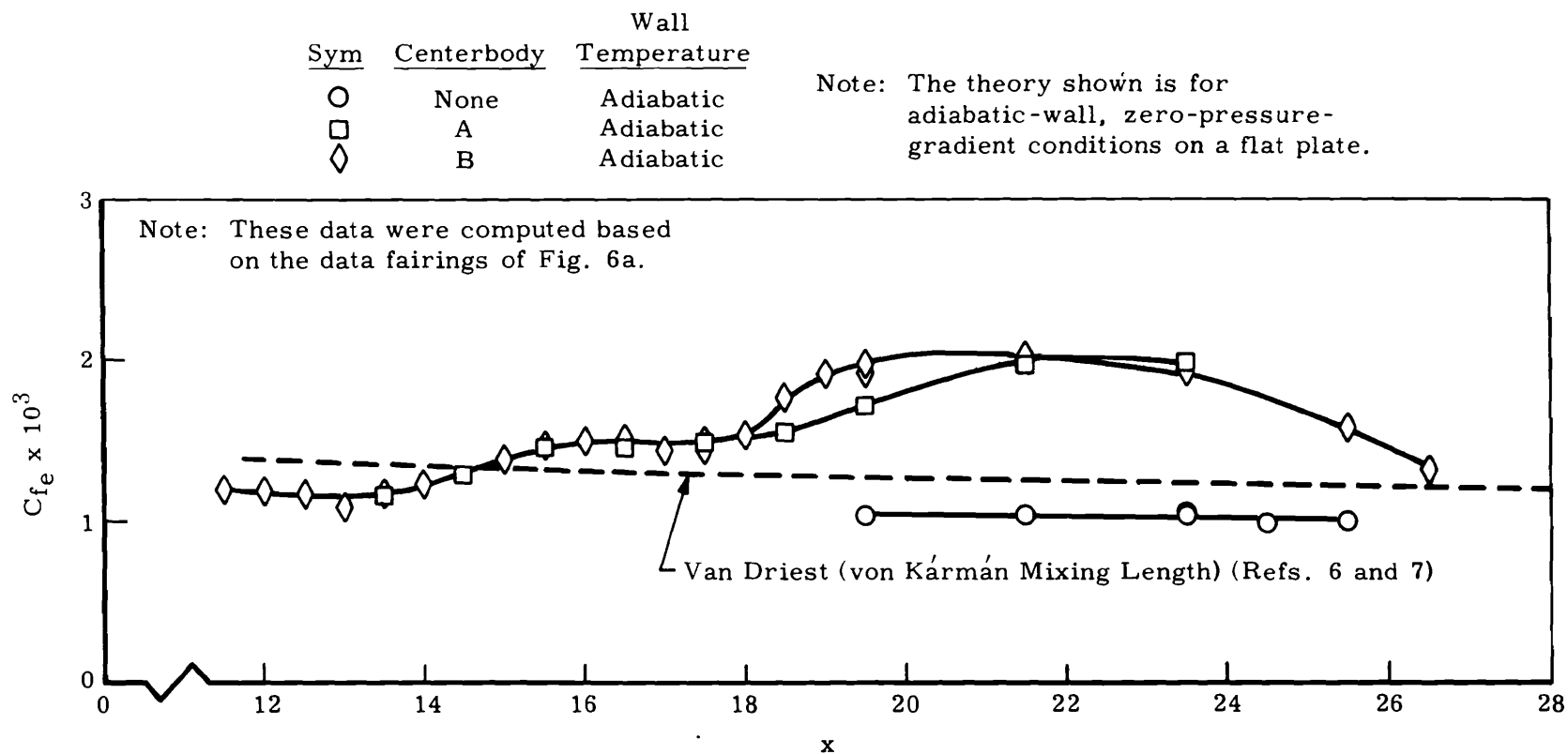
b. Based on Local Conditions
Fig. 6 Concluded

Note: The theory shown is for zero-pressure-gradient conditions on a flat plate with $T_W/T_O = 0.3$ and $M_\infty = 4.0$.

Sym	Centerbody	Wall Temperature
◇	A	Cold
◆	B	Cold
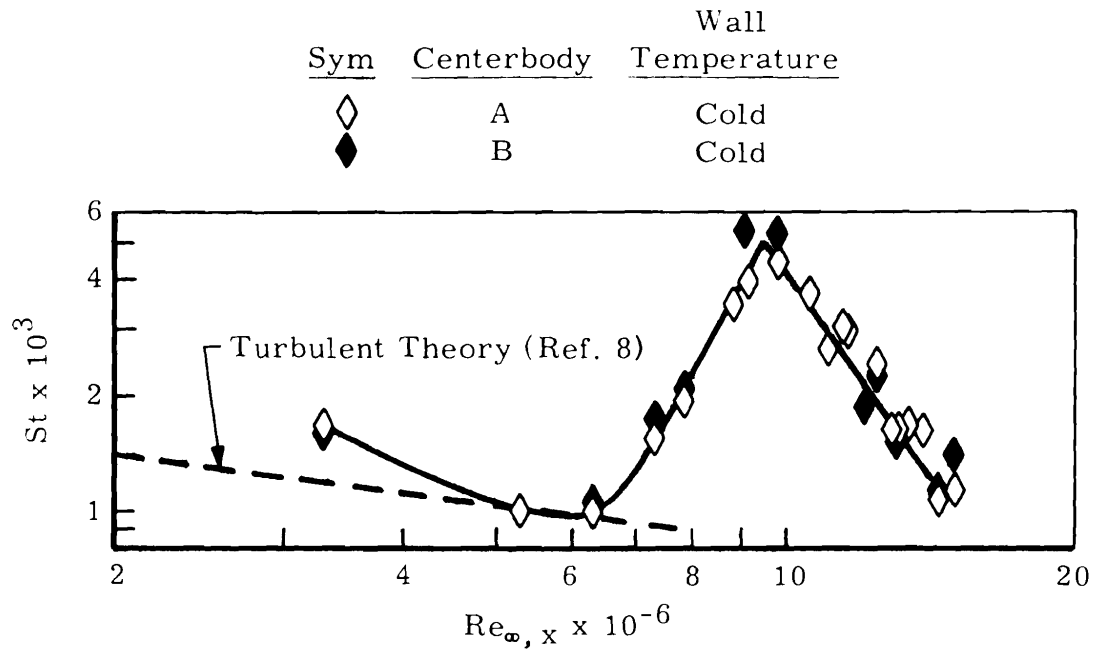
Fig. 7 Heat-Transfer Distributions along the Wall
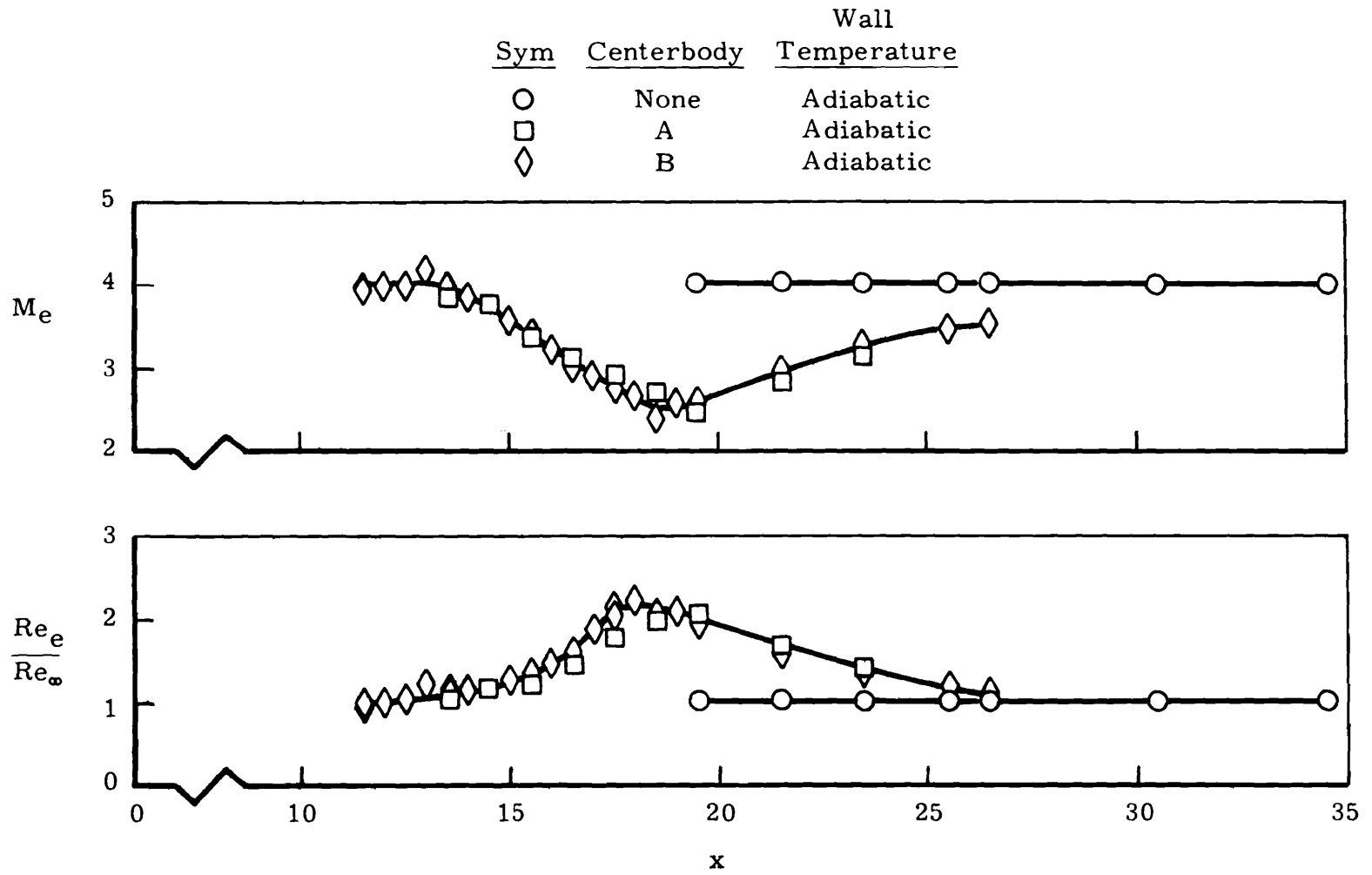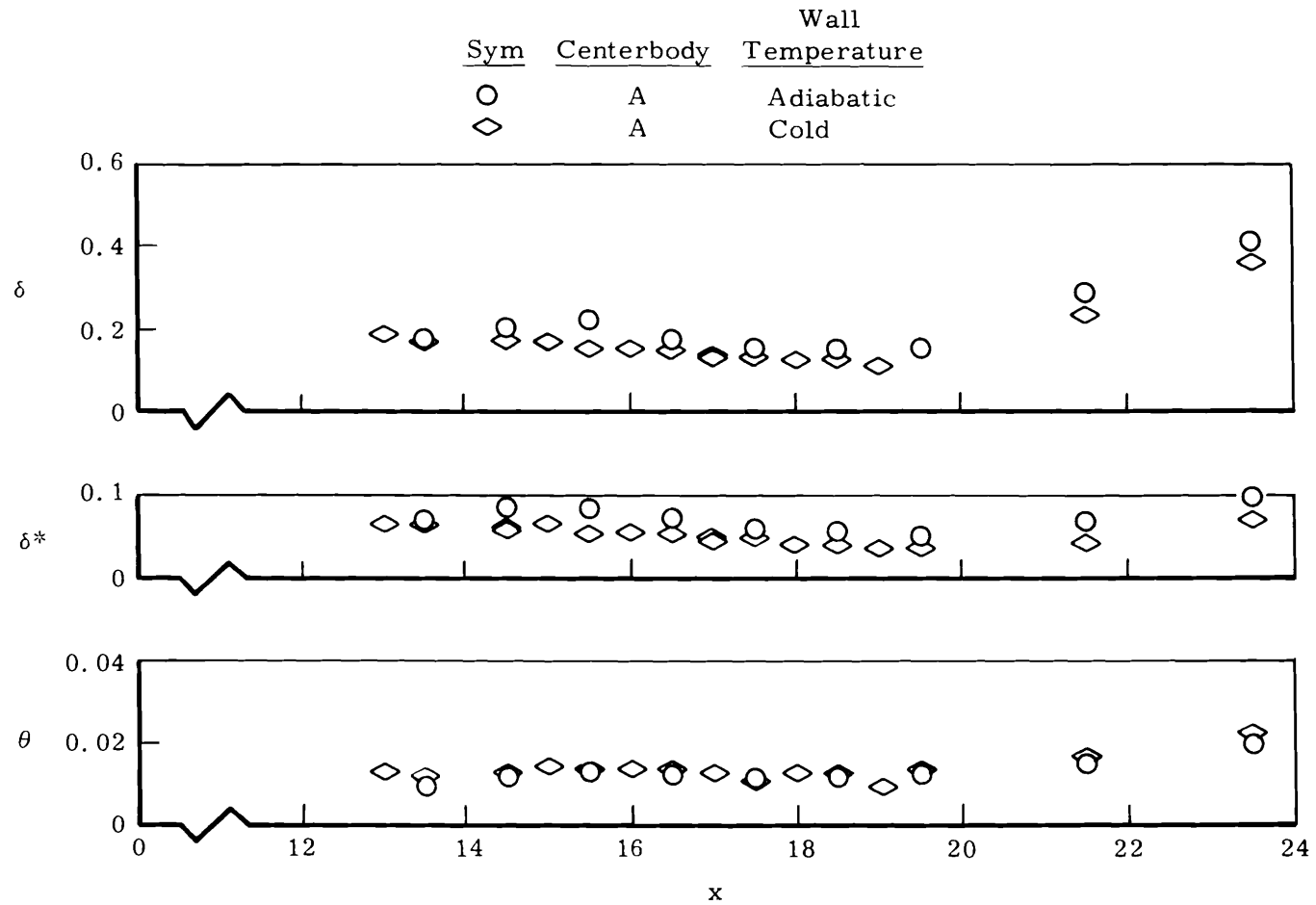
a. Pressure Gradient Effects
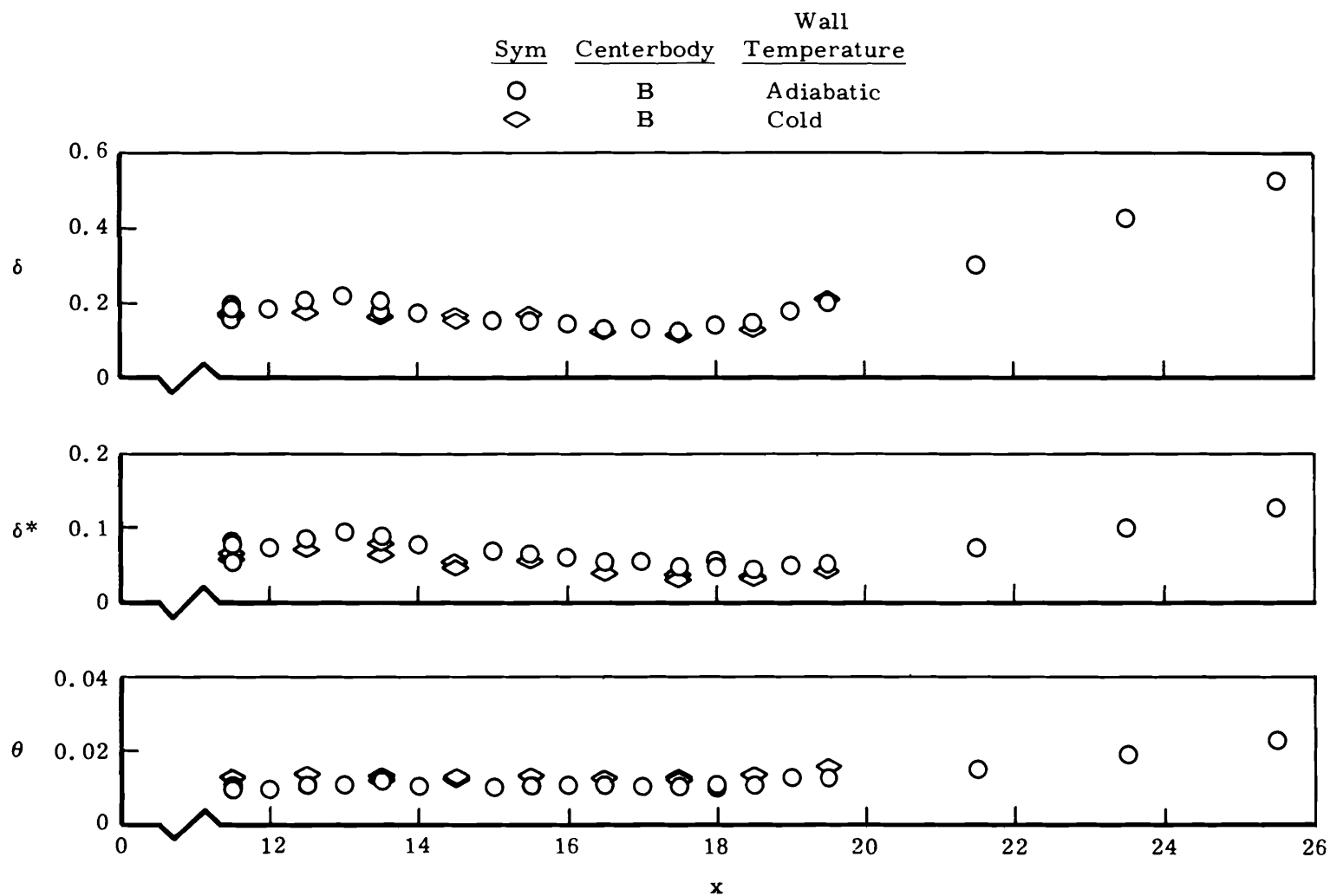Fig. 8 Local Flow Conditions
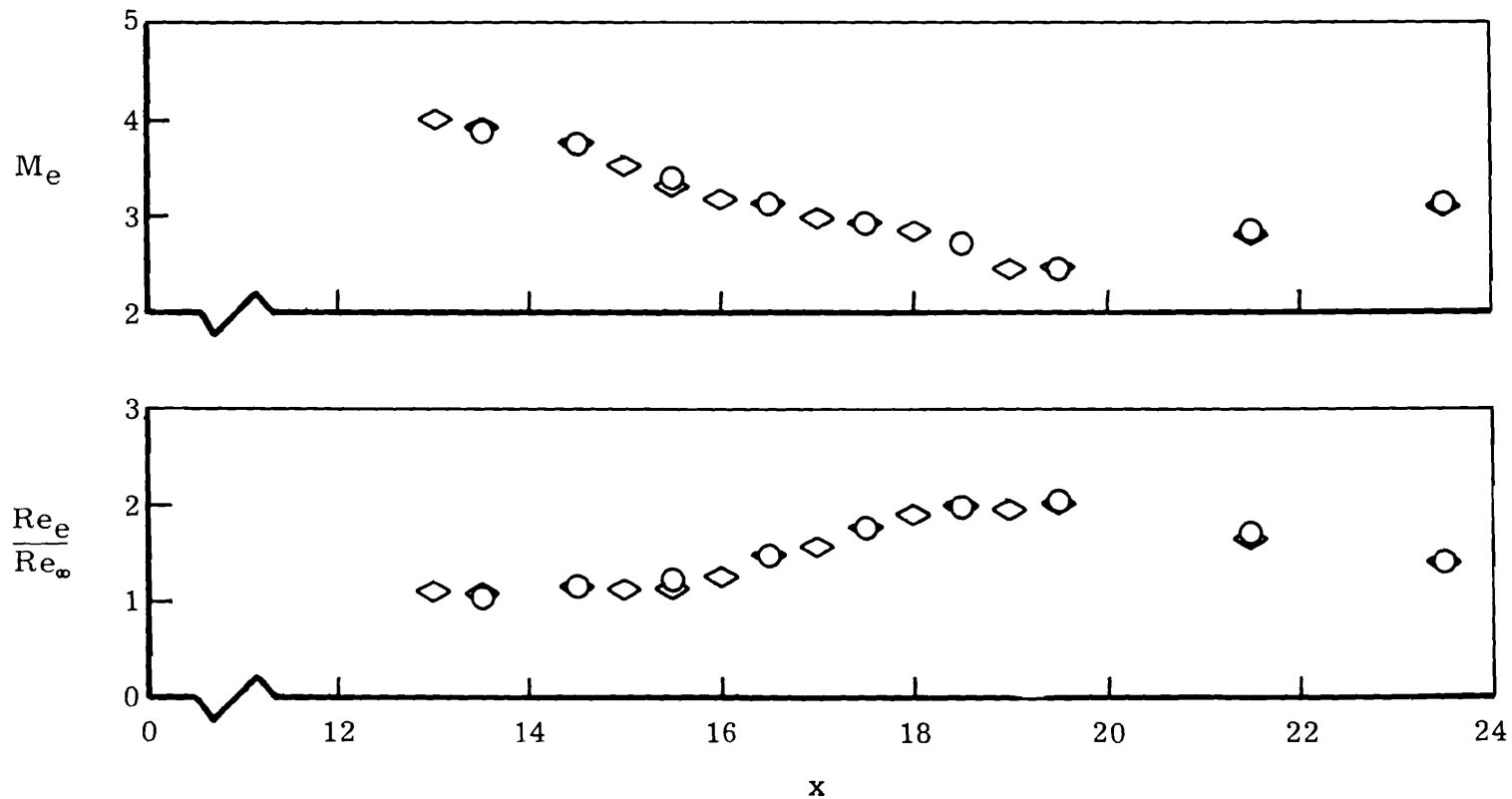
b. Wall Temperature Effects

Fig. 8 Concluded

Sym	Centerbody	Wall Temperature
O	None	Adiabatic
□	A	Adiabatic
◇	B	Adiabatic
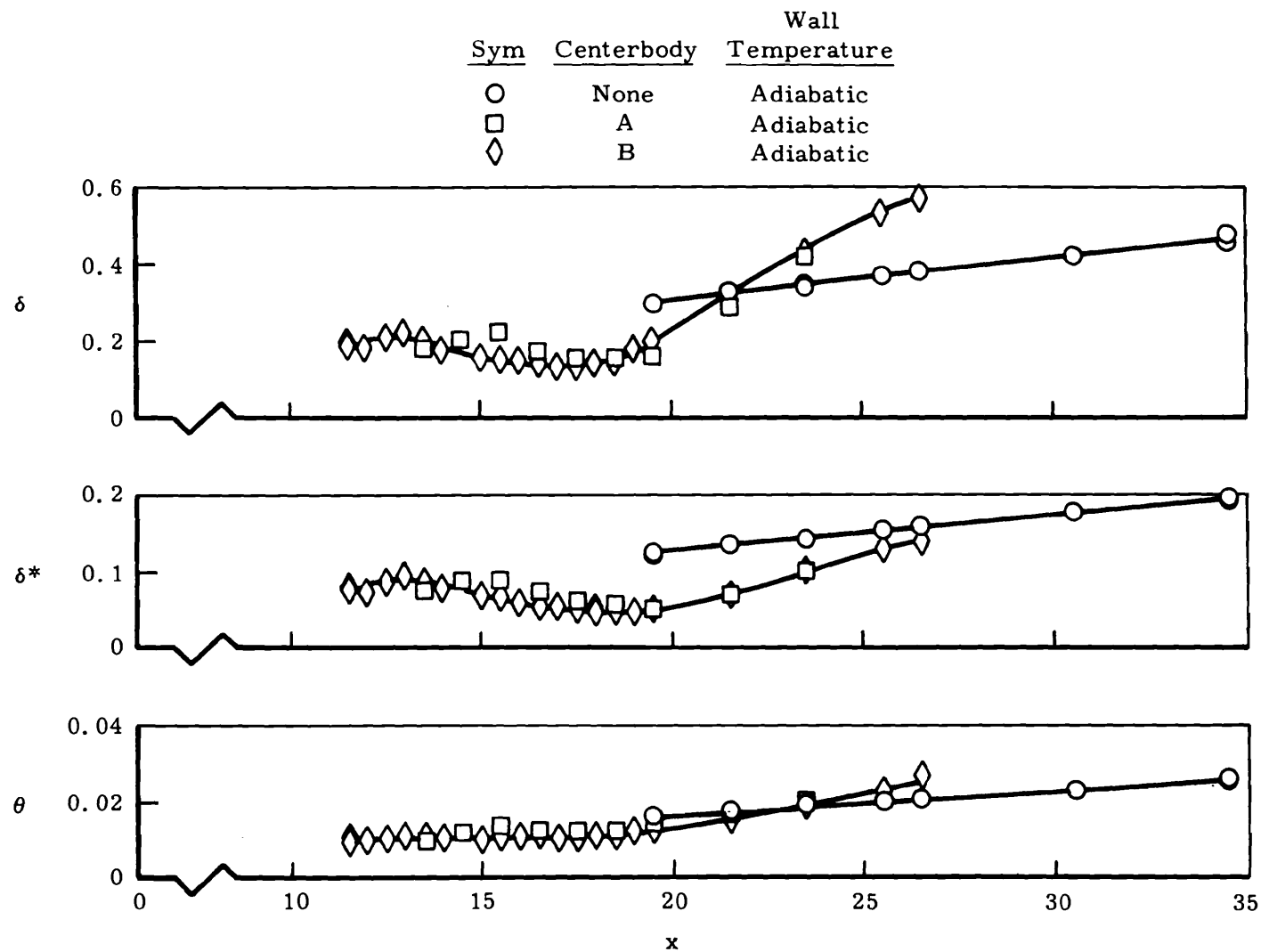
a. Pressure Gradient Effects

Fig. 9 Boundary-Layer Parameters

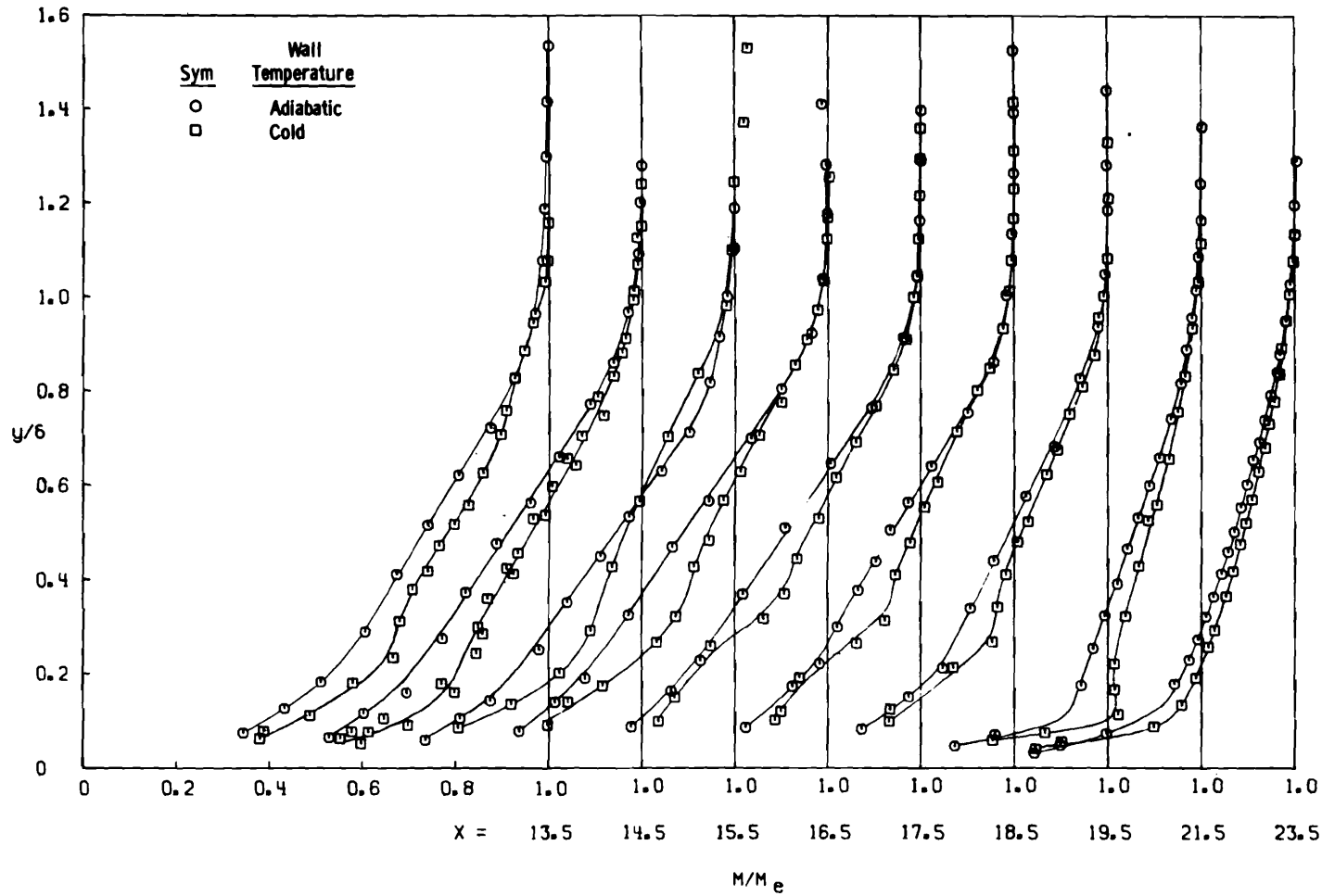b. Wall Temperature Effects for Centerbody A
Fig. 9 Continued

Sym	Centerbody	Wall Temperature
○	B	Adiabatic
◇	B	Cold

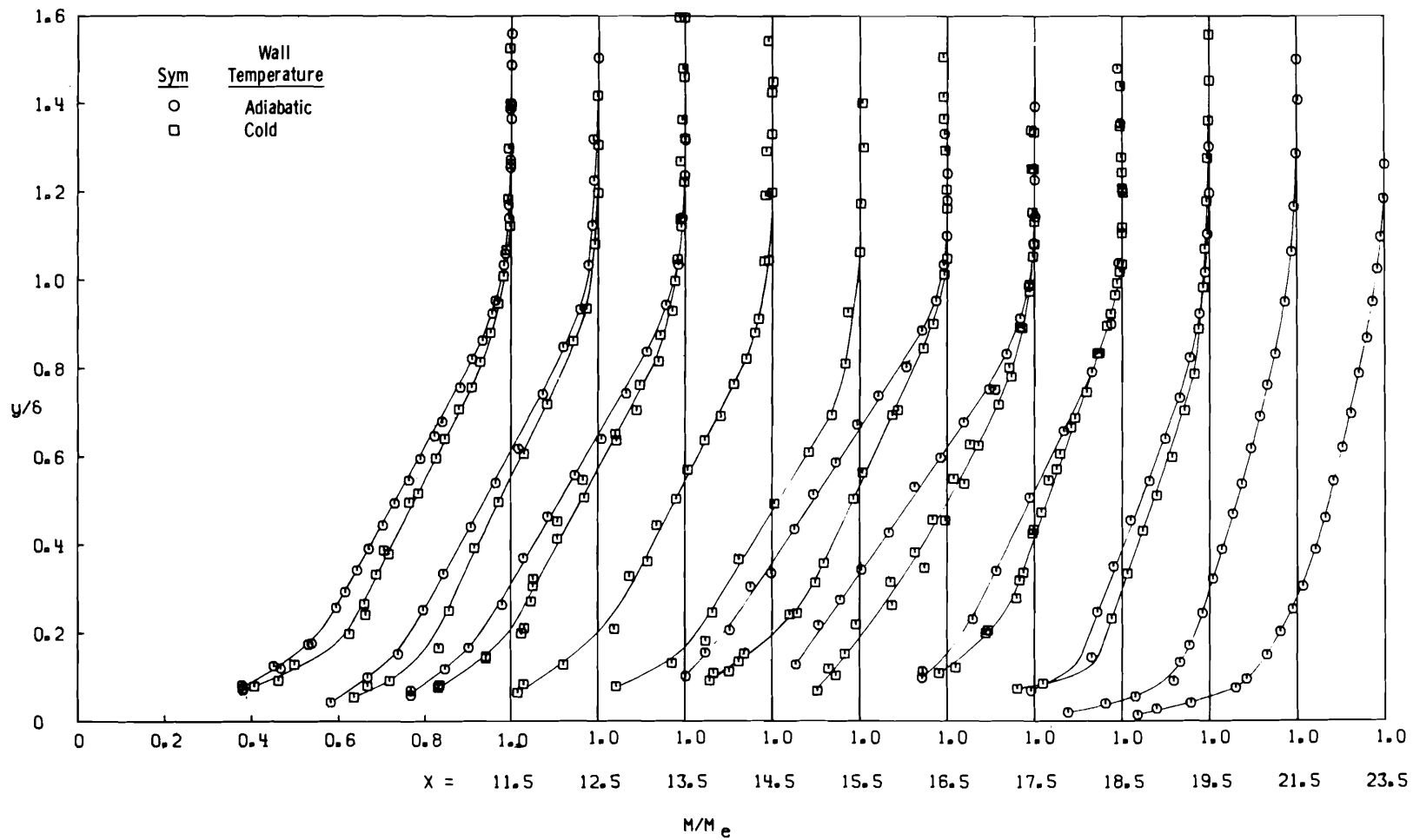c. Wall Temperature Effects for Centerbody B
Fig. 9 Continued
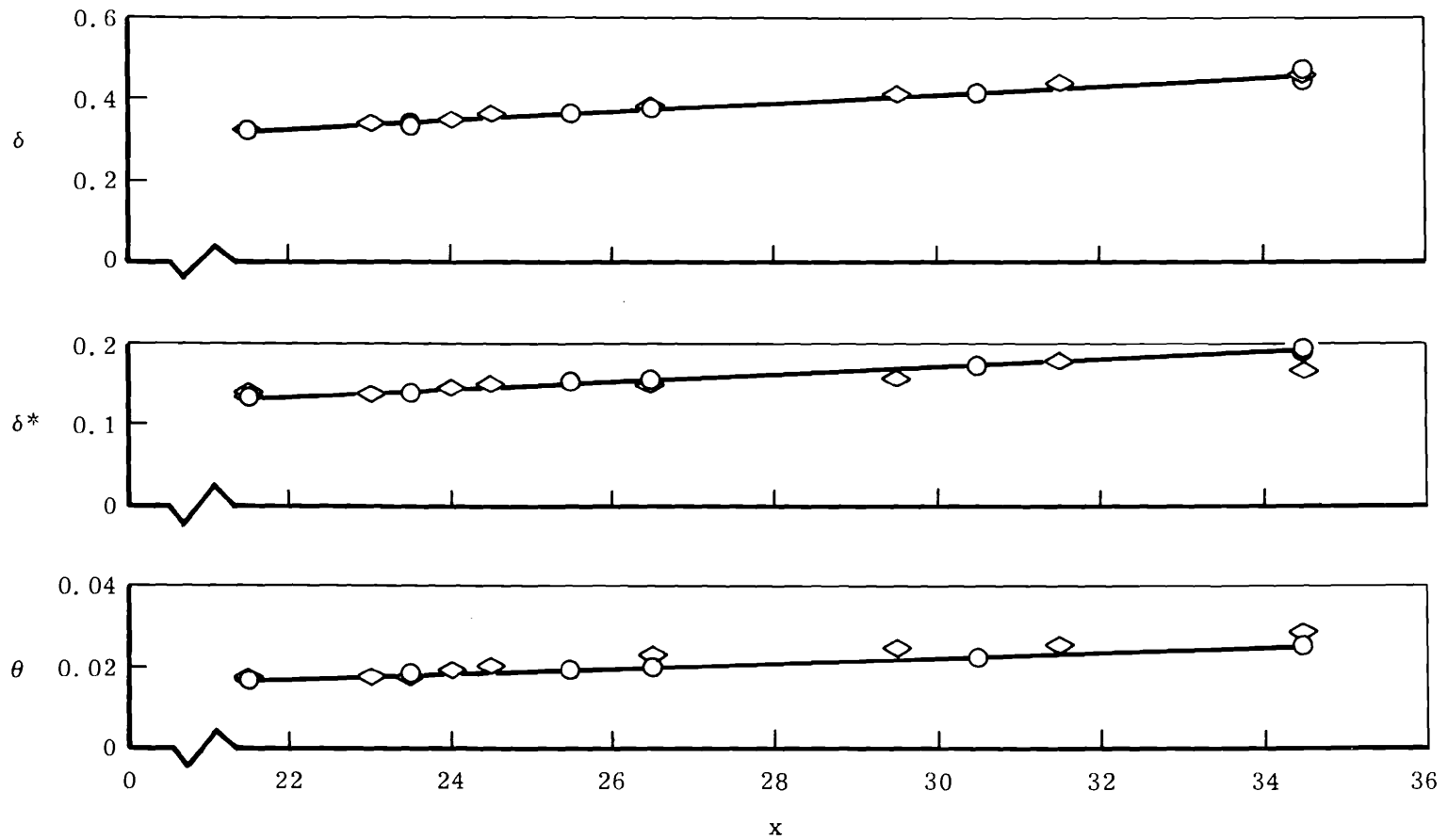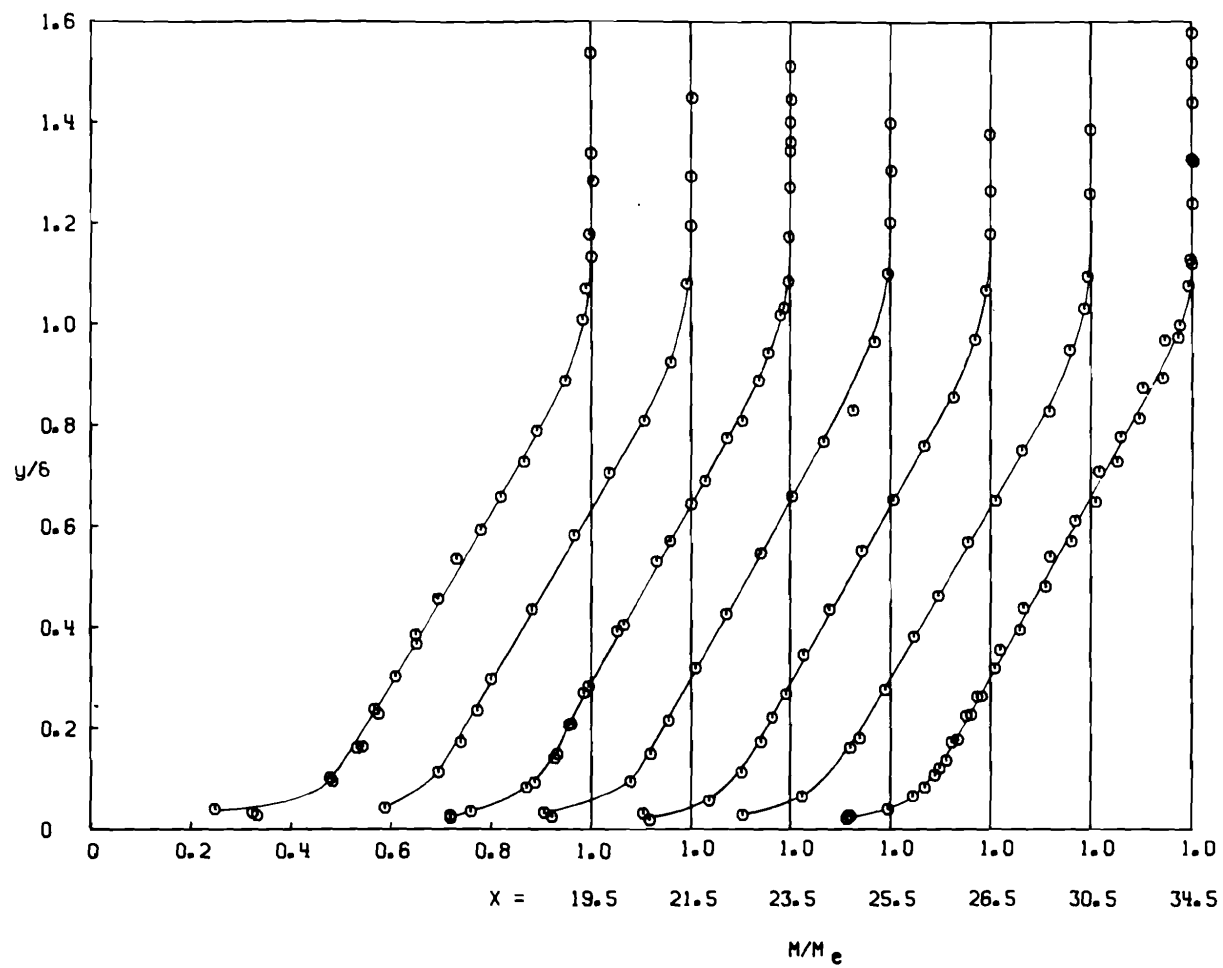
d. Step-Down Temperature Effects
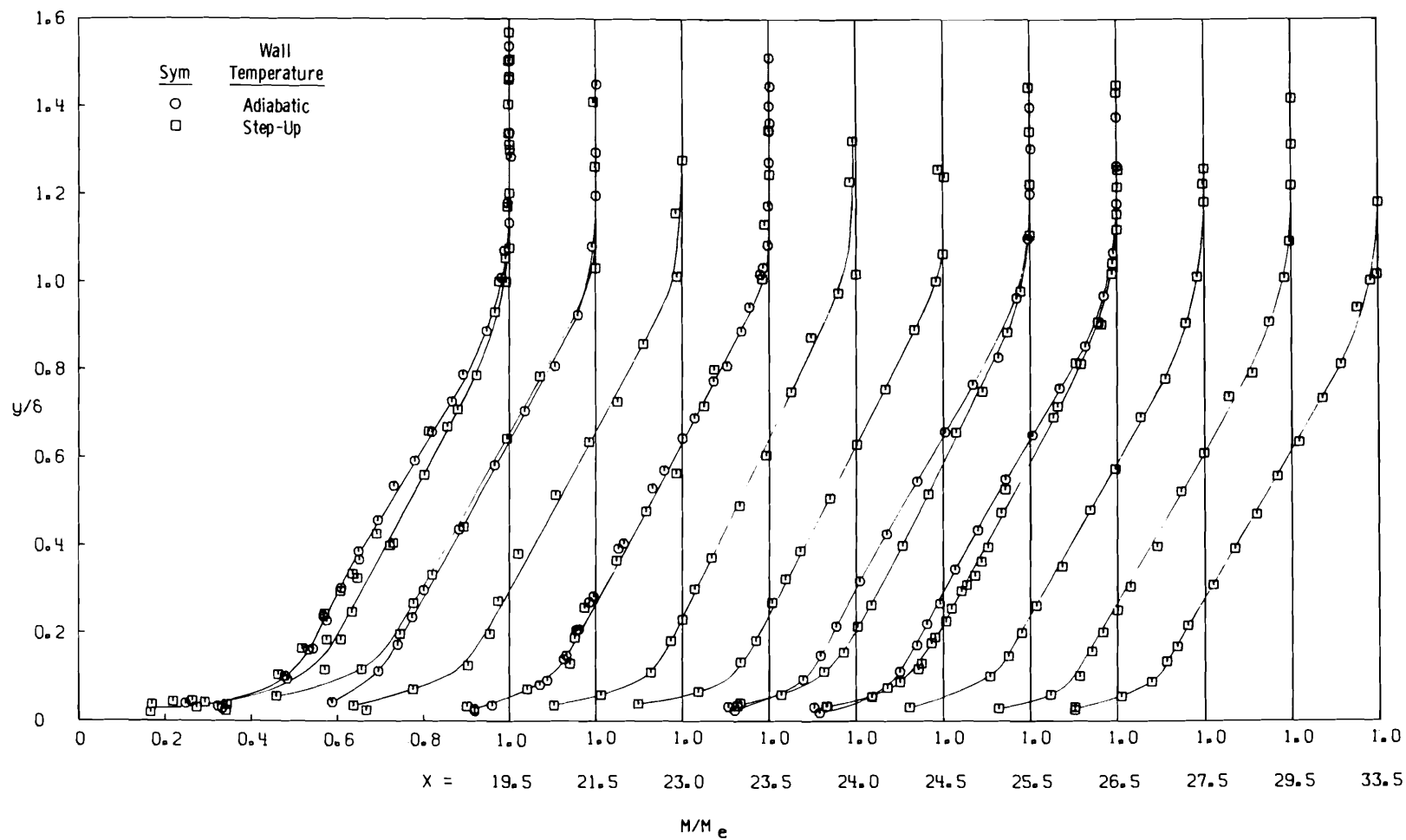Fig. 9 Concluded

a. Centerbody A

Fig. 10 Mach Number Profiles at Various Model Wall Stations

b. Centerbody B
Fig. 10 Continued

c. No Centerbody, Adiabatic Wall Temperature
Fig. 10 Continued

d. No Centerbody, Step-Up Wall Temperature
Fig. 10 Continued

e. No Centerbody, Step-Down Wall Temperature
Fig. 10 Concluded

a. Centerbody A

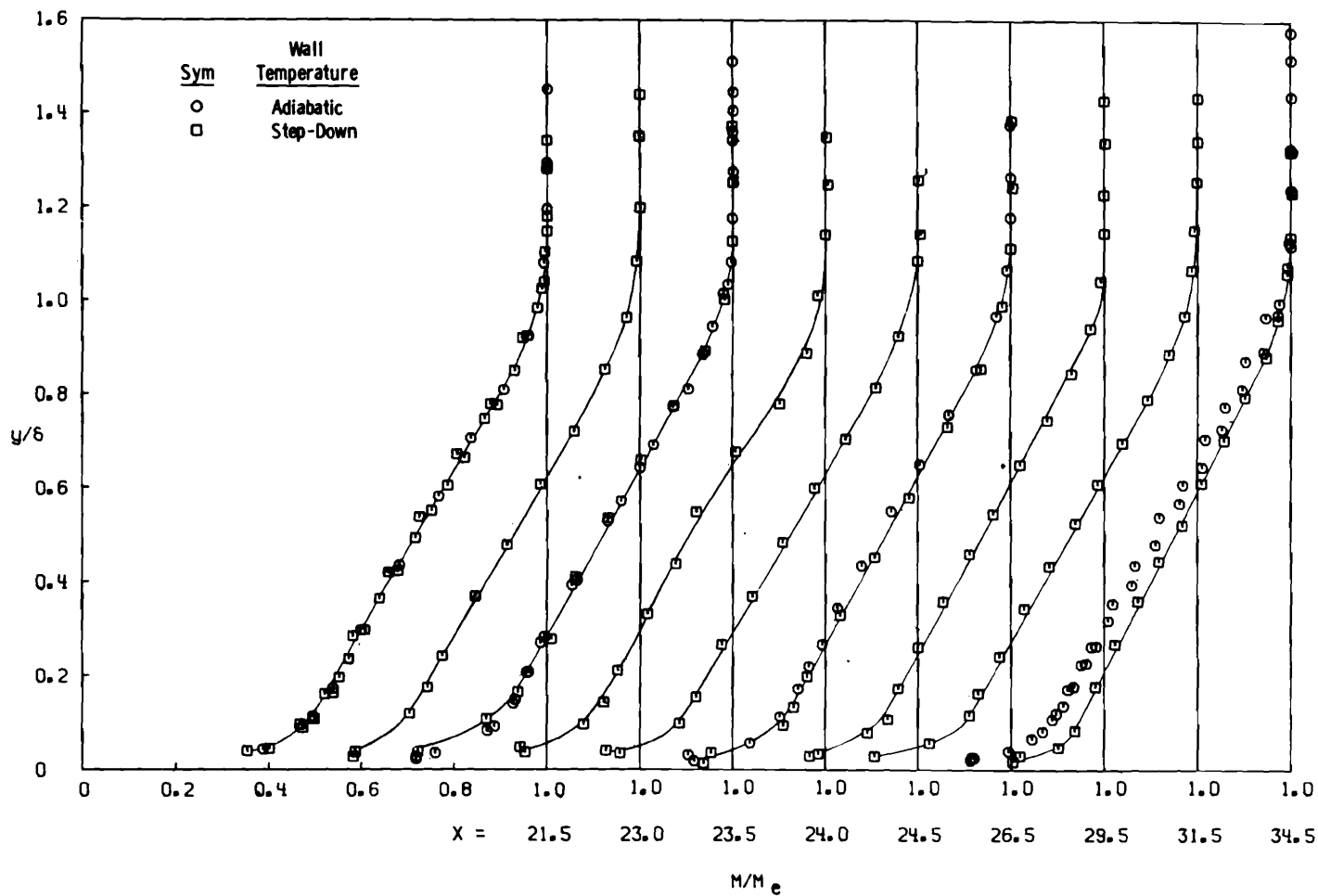Fig. 11 Total Temperature Profiles at Various Model Wall Stations
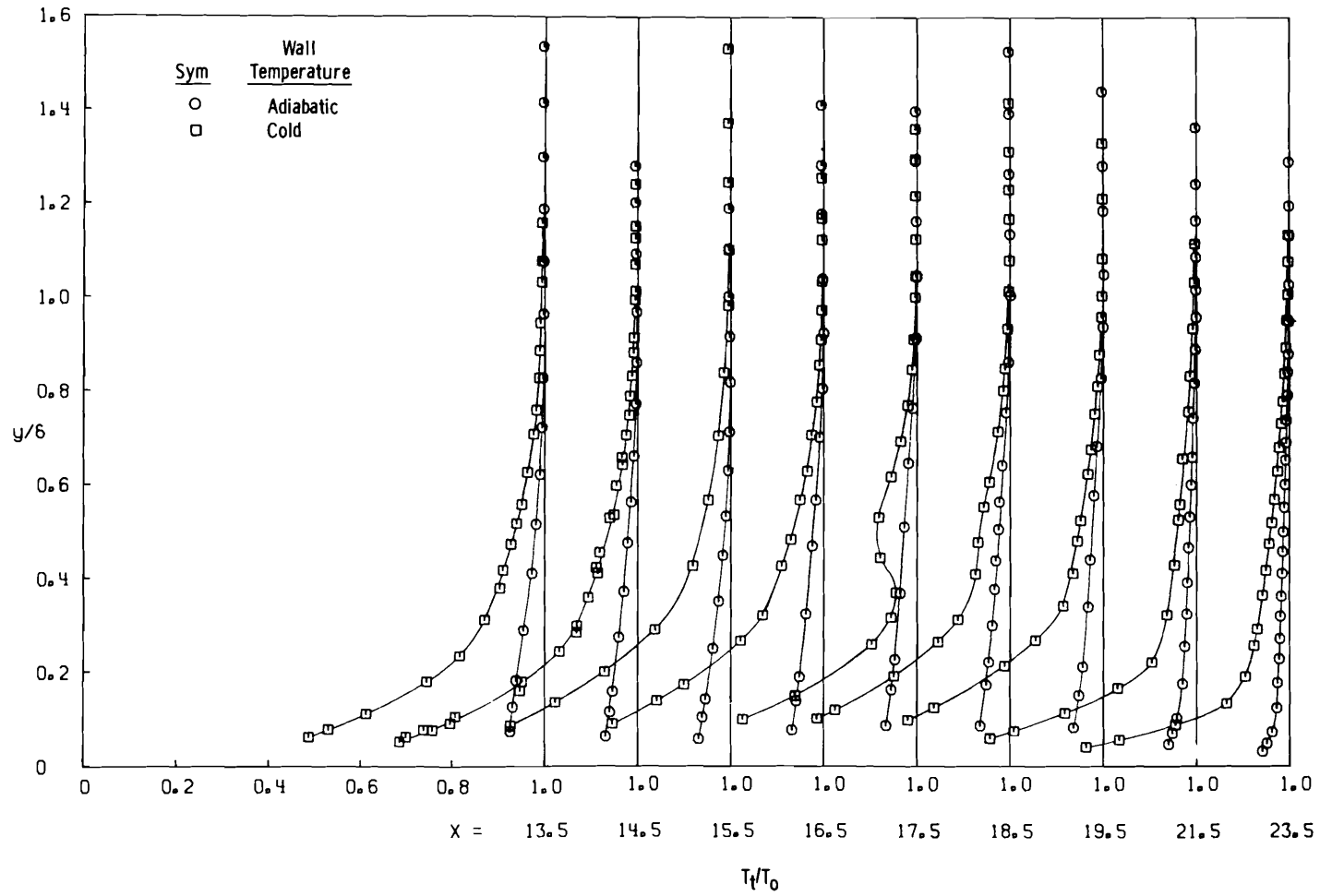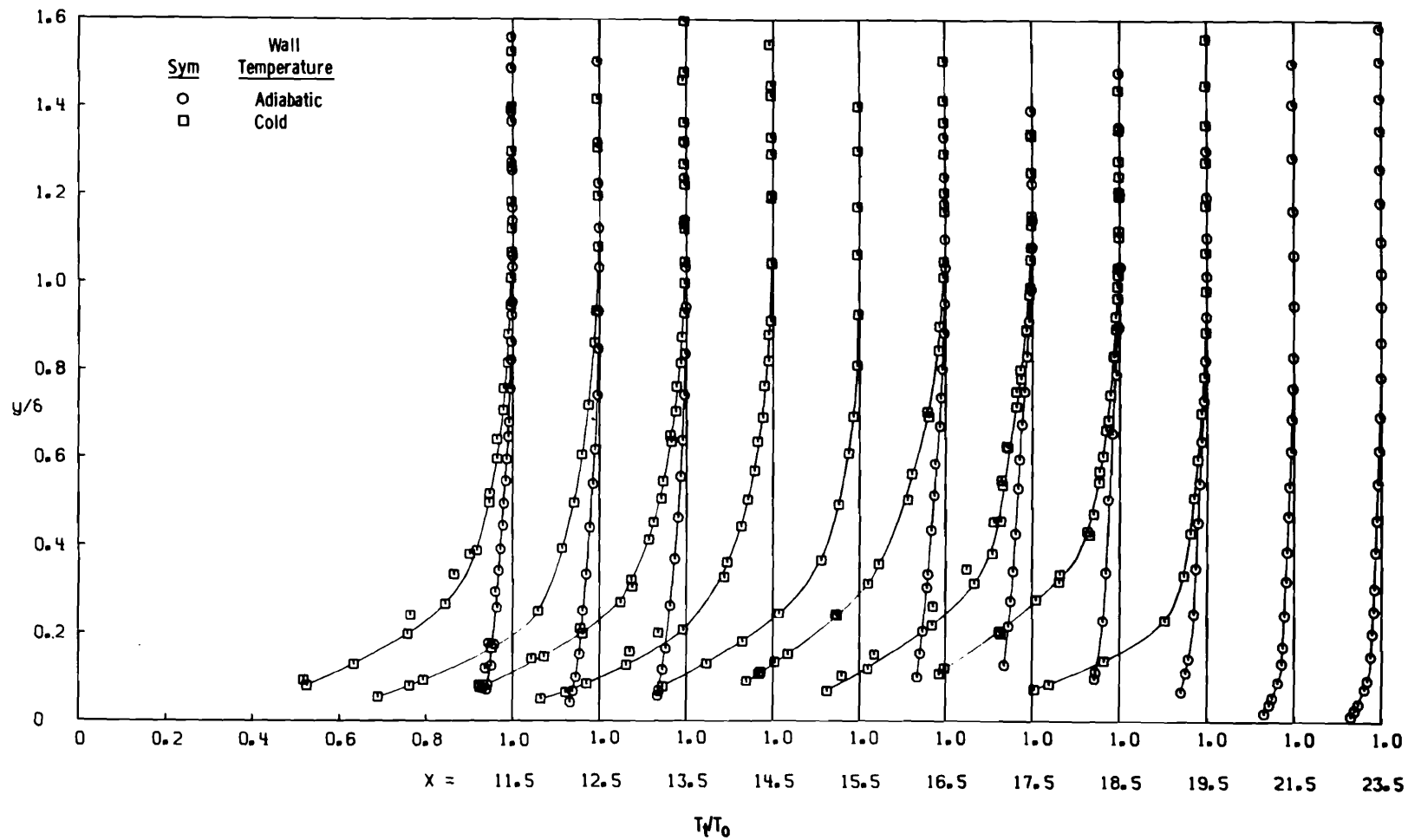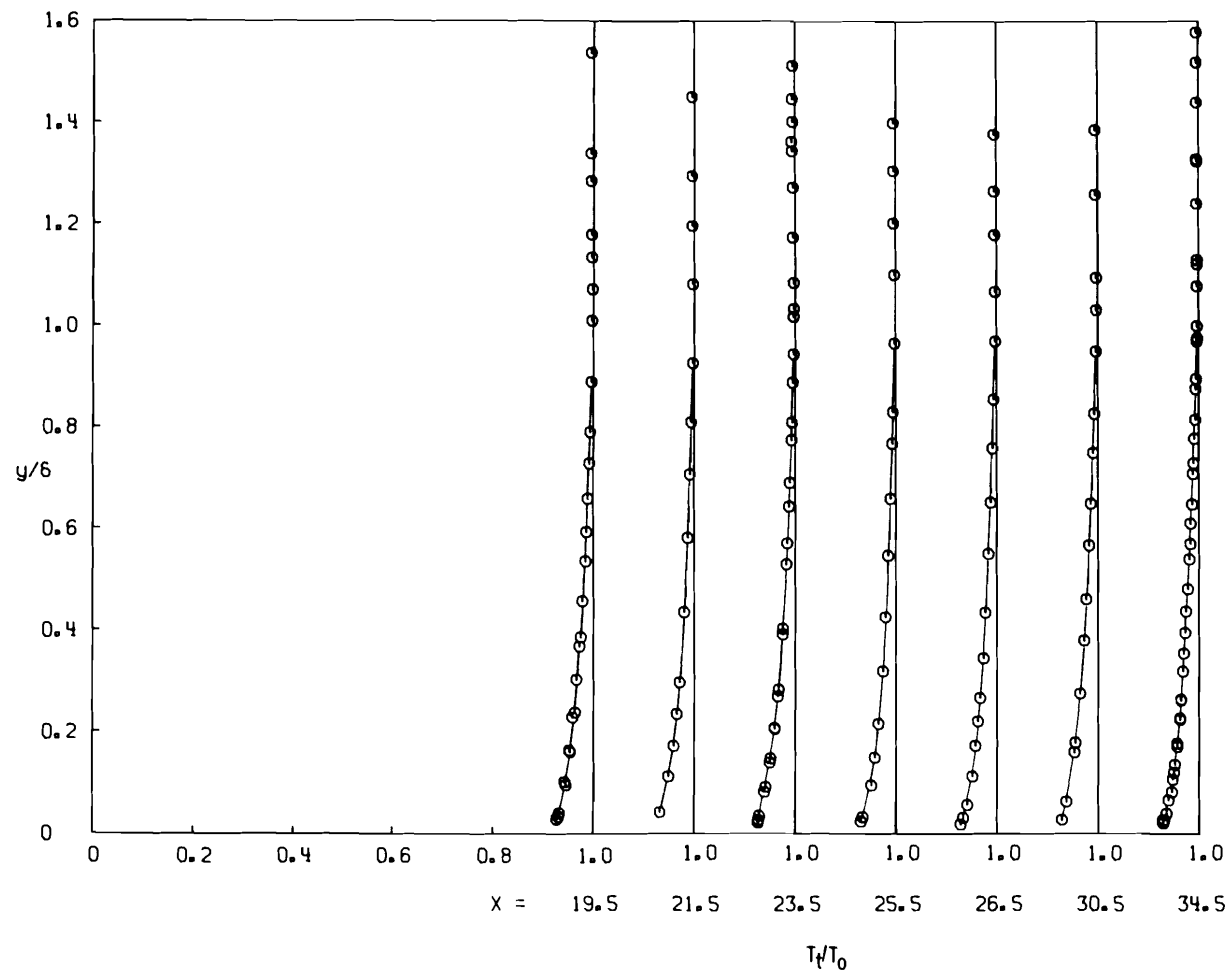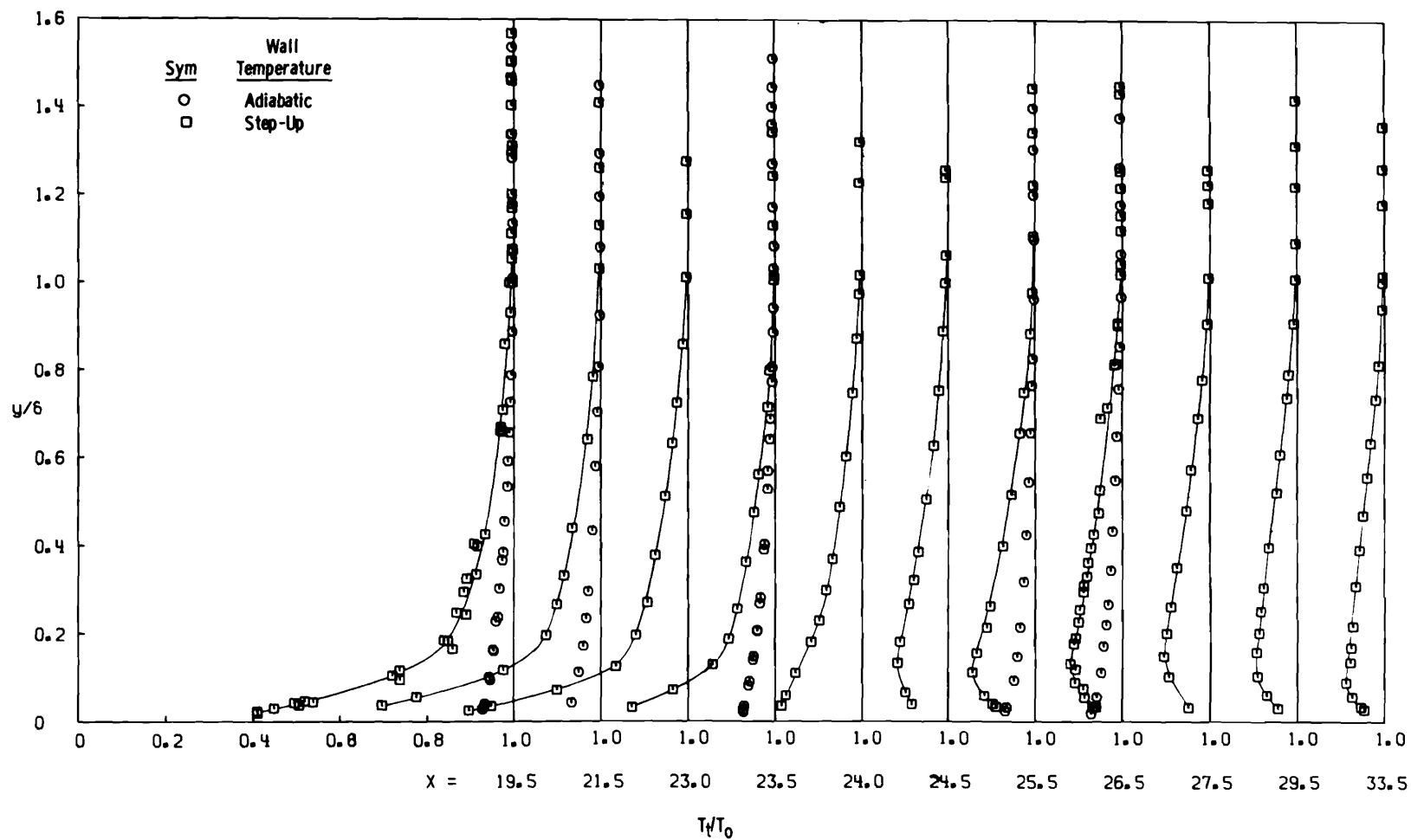
b. Centerbody B
Fig. 11 Continued

c. No Centerbody, Adiabatic-Wall Temperature

Fig. 11 Continued

d. No Centerbody, Step-Up Wall Temperature
Fig. 11 Continued
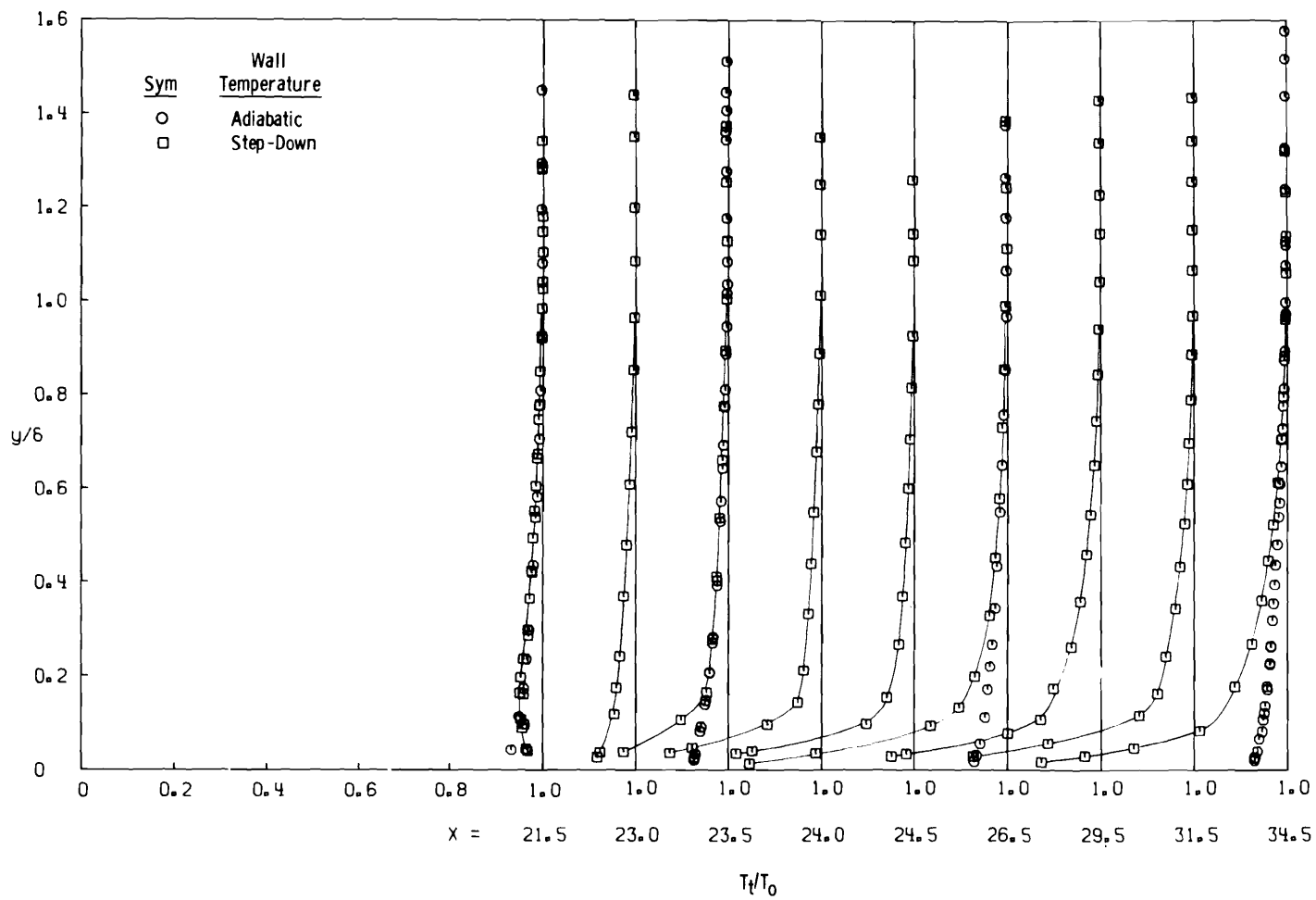
e. No Centerbody, Step-Down Wall Temperature

Fig. 11 Concluded

Centerbody A

Centerbody B

Sym	x	Pressure Gradient	Centerbody
O	11.5	None	B
△	15.5	Adverse	A
□	16.5	Adverse	A
◇	17.5	Adverse	A
×	19.5	Favorable	A
+	21.5	Favorable	A
⋈	23.5	Favorable	A

Sym	x	Pressure Gradient	Centerbody
O	11.5	None	B
□	16.5	Adverse	B
◇	17.5	Adverse	B
×	19.5	Favorable	B
+	21.5	Favorable	B
⋈	23.5	Favorable	B

y/δ

M/M_e
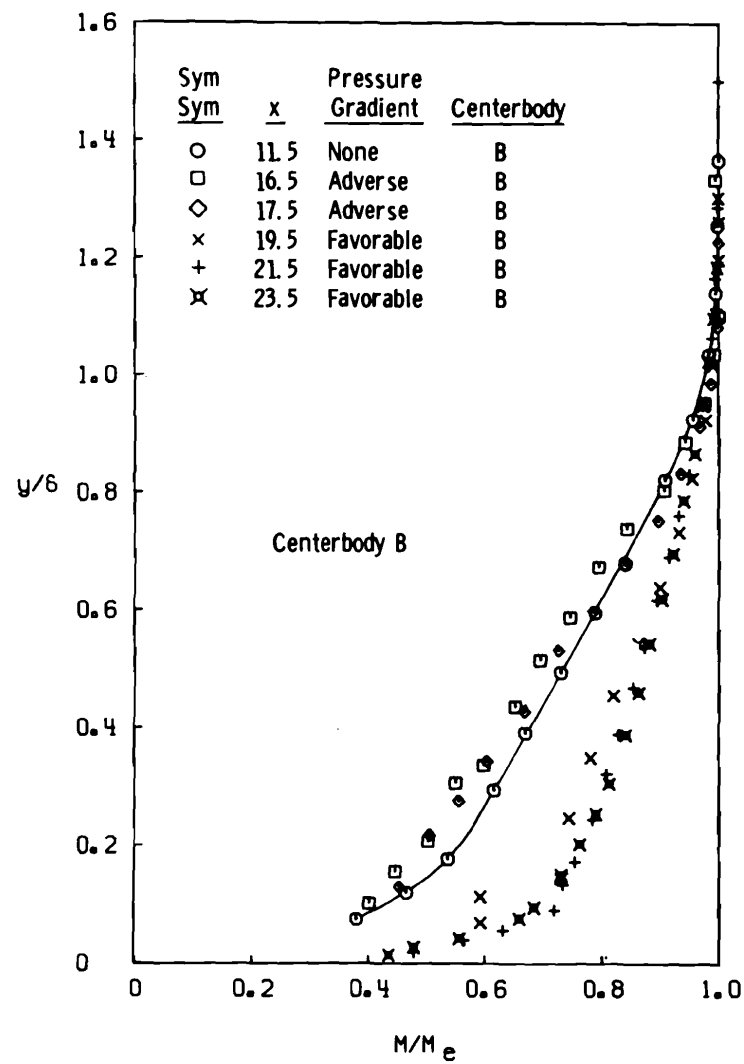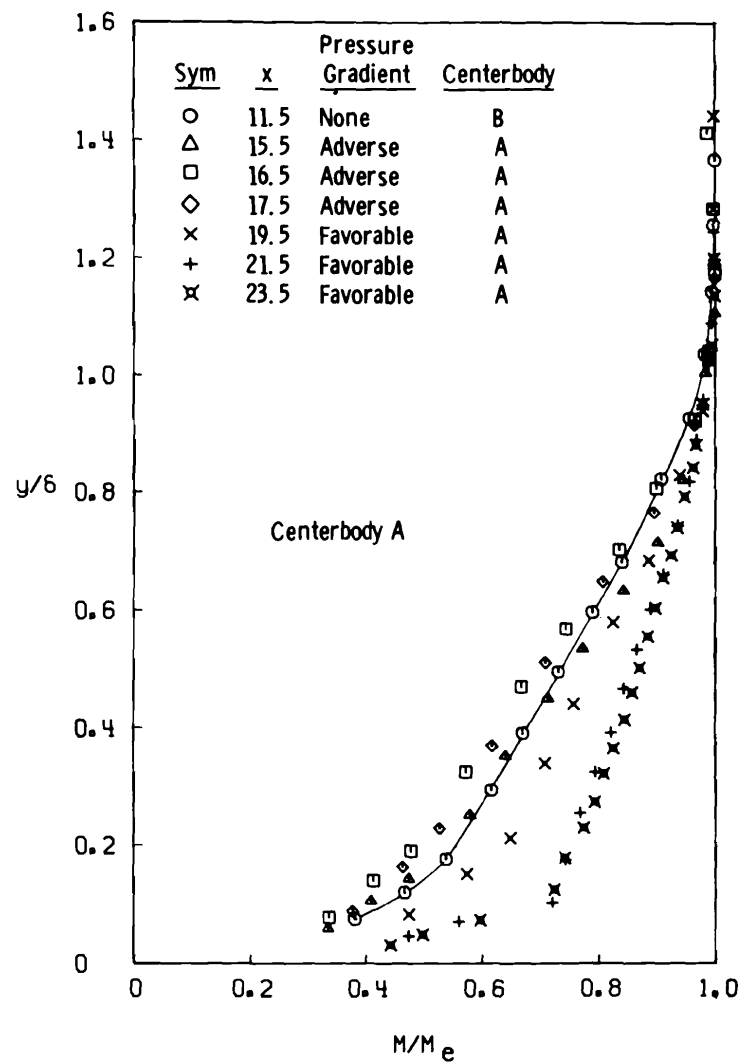
a.   For Adiabatic-Wall Conditions

Fig. 12 Pressure Gradient Effects on Boundary-Layer Mach Number Profiles
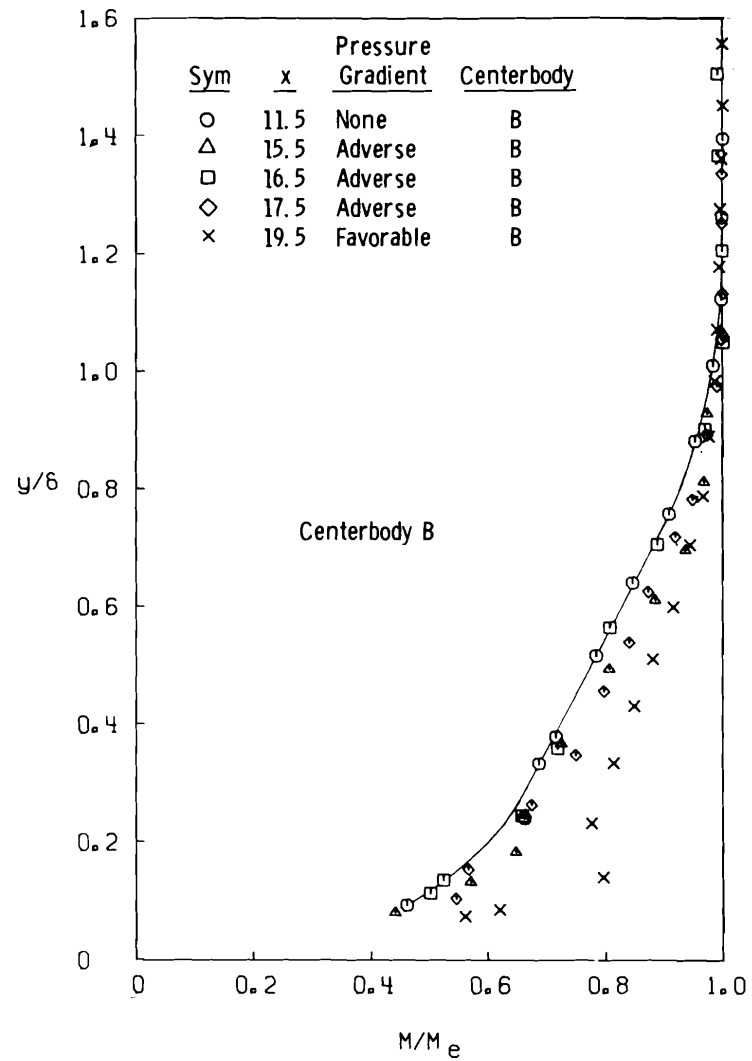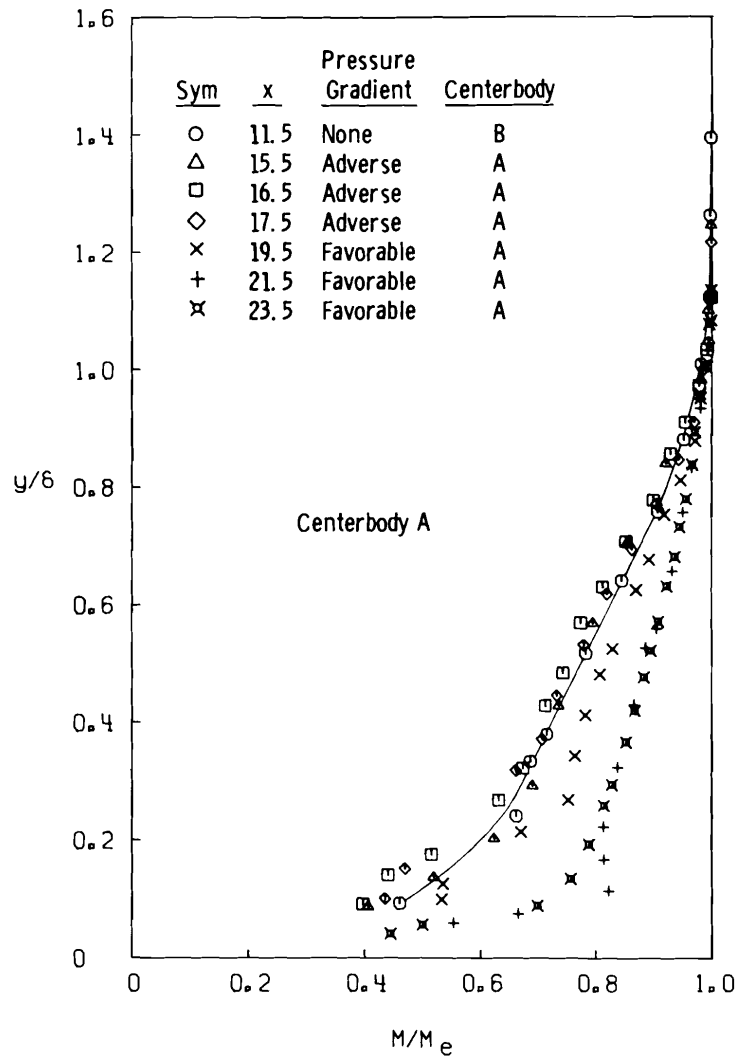
b. For Cold-Wall Conditions
Fig. 12 Concluded

Fig. 13 Step-Down Wall Temperature Effects on Boundary-Layer Mach Number Profiles

TABLE I
INSTRUMENTATION LOCATIONS

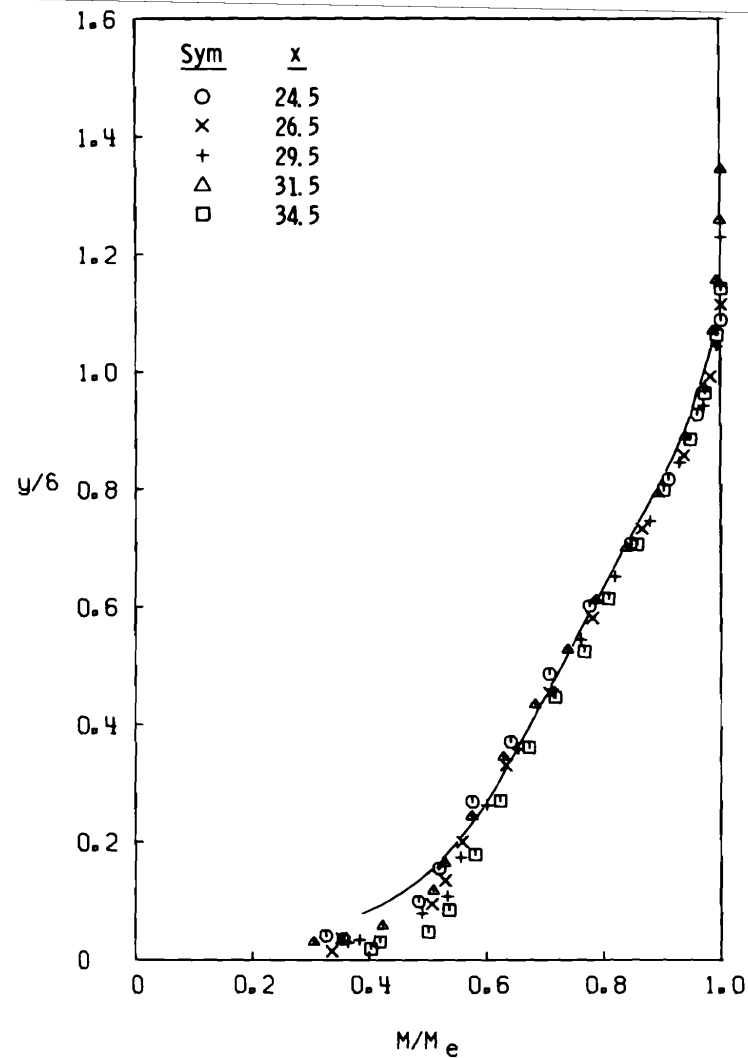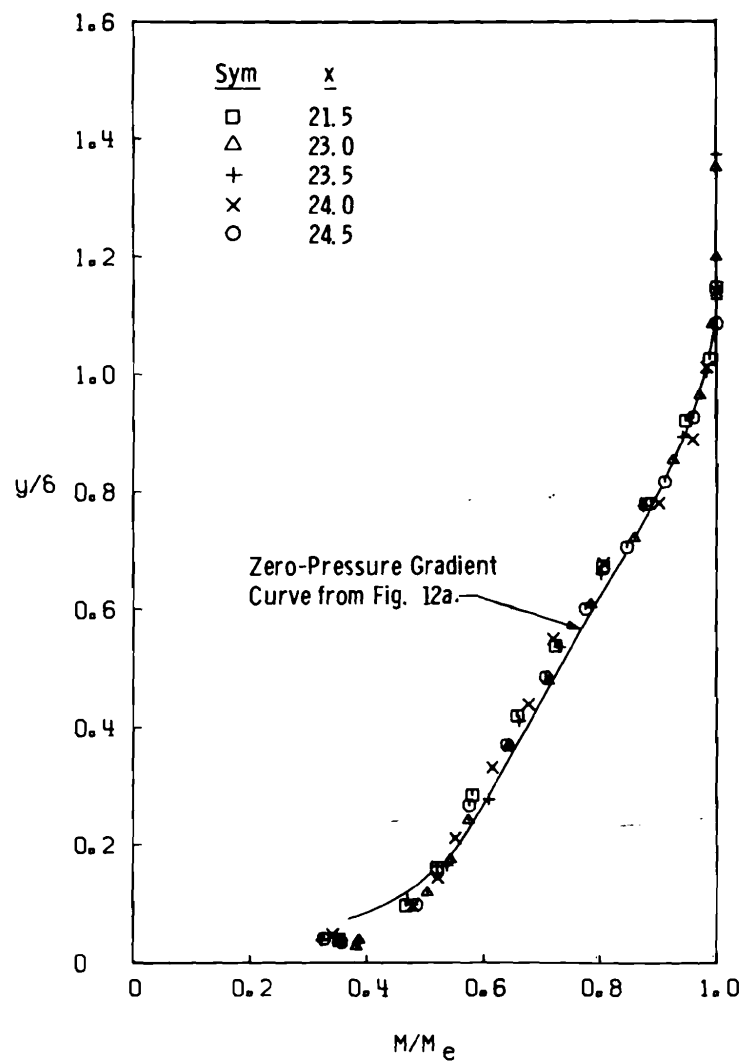| x, in.	φ, deg					
	-8.6	-5.7	-4.3	0	4.3	8.6
2.482	S	GT		P*	T	
3.482				P		S
4.482	S	GT				
5.482	S					S
6.482	S	GT				
7.482			T			S
8.482	S	GT				
9.482						S
10.482	S	GT				
11.482						S
12.482	S	GT			T	
13.482						S
14.482	S	GT*				
14.982						
15.482		GT				S
15.982						
16.482	S	GT				
16.982				↓		
17.482		GT	T	P*		S
17.982				P		
18.482	S	↓				
18.982						
19.482		G				S
19.982						
20.482	S	↓		↓		

x, in.	φ, deg					
	-8.6	-5.7	-4.3	0	4.3	8.6
20.982		G		P		
21.482		G				S
21.982		G				
22.482	S	GT			T	
22.982						
23.482						S
23.982						
24.482	S					
24.982						
25.482				↓		S
25.982						
26.482	S	GT*		P*		S
27.482		GT	T	P		S
28.482	S	↓				
29.482	S	↓				S
30.482	S					
31.482		GT				S
32.482	S				T	
33.482	S	GT				S
34.482	S			↓		
35.482	S	GT		P*		S
36.482	S			P		
37.482		GT	T			S
38.482	S					
39.482		GT		↓		S

G: Gardon gage without temperature
GT: Gardon gage with temperature
P: Static pressure tap
S: Stanton tube
T: Chromel-Alumel thermocouple

P*: Static pressure taps are also located at
φ = 45, 90, 135, 180, 225, 270, and 315 deg

GT*: Gardon gages with temperatures are also
located at x = 14.66, 14.98, and 15.20 in.
or at x = 27.20, 27.44, and 27.75 in. for
φ = 90, 180, and 270 deg, respectively.

TABLE II
TEST SUMMARY

Centerbody	Wall Temperature	Nominal Model Station, x, in.		
		Boundary-Layer Survey Data	Model Surface Data	
			Minimum	Maximum
None	Adiabatic	19.5, 21.5, 23.5, 25.5, 26.5, 30.5, 34.5,	2.5	39.5
	Adiabatic*	11.5, 19.5, 26.5		
	Step-Up**	19.5, 21.5, 23.0, 23.5, 24.0, 24.5, 25.5, 26.5, 27.5, 29.5, 31.5, 33.5, 35.5		
	Step-Down	21.5, 23.0, 23.5, 24.0, 24.5, 26.5, 29.5, 31.5, 34.5		
A(β = 4)	Adiabatic	13.5, 14.5, 15.5, 16.5, 17.5, 18.5, 19.5, 21.5, 23.5		32.5
	Cold	13.0, 13.5, 14.5, 15.0, 15.5, 16.0, 16.5, 17.0, 17.5, 18.0, 18.5, 19.0, 19.5, 21.5, 23.5		
B(β = 6)	Adiabatic	11.5, 12.5, 13.5, 15.5, 16.5, 17.5, 18.5, 19.5		
	Adiabatic*	9.5, 11.5, 12.0, 12.5, 13.0, 13.5, 14.0, 14.5, 15.0, 15.5, 16.0, 16.5, 17.0, 17.5, 18.0, 18.5, 19.0, 19.5, 21.5, 23.5, 25.5, 26.5		
	Cold	11.5, 12.5, 13.5, 14.5, 15.5, 16.5, 17.5, 18.5, 19.5		
	Cold**	11.5*, 12.5, 13.5, 14.5, 15.5, 16.5, 17.0*, 17.5, 18.0, 18.5, 19.5, 21.5, 23.5, 26.5		

* Data obtained using only one linear potentiometer
** Data obtained without using the frost-elimination technique

DOCUMENT CONTROL DATA - R & D		
(Security classification of title, body of abstract and indexing annotation must be entered when the overall report is classified)		

1. ORIGINATING ACTIVITY *(Corporate author)*	2a. REPORT SECURITY CLASSIFICATION
Arnold Engineering Development Center ARO, Inc., Operating Contractor Arnold Air Force Station, Tennessee 37389	UNCLASSIFIED
	2b. GROUP
	N/A

3. REPORT TITLE

EXPERIMENTAL INVESTIGATION OF TURBULENT BOUNDARY LAYERS WITH PRESSURE GRADIENT AND HEAT TRANSFER AT MACH NUMBER 4

4. DESCRIPTIVE NOTES *(Type of report and inclusive dates)*

Final Report   July 13 to August 26, 1970

5. AUTHOR(S) *(First name, middle initial, last name)*

J. S. Hahn and Ronald G. Lutz, ARO, Inc.

6. REPORT DATE	7a. TOTAL NO. OF PAGES	7b. NO. OF REFS
January 1971	57	8

8a. CONTRACT OR GRANT NO.	9a. ORIGINATOR'S REPORT NUMBER(S)
F40600-71-C-0002	
b. PROJECT NO.	AEDC-TR-71-3
c. Program Element 63311F	9b. OTHER REPORT NO(S) *(Any other numbers that may be assigned this report)*
d. System 627A	ARO-VKF-TR-70-296

10. DISTRIBUTION STATEMENT Each transmittal of this document outside the Department of Defense must have prior approval of SAMSO/TRD-STINFO, AF Unit Post Office, Los Angeles, California 90045.

11. SUPPLEMENTARY NOTES	12. SPONSORING MILITARY ACTIVITY
Available in DDC.	SAMSO, AFSC, AF Unit Post Office, Los Angeles, California 90045

13. ABSTRACT

An experimental investigation of the behavior of a turbulent boundary layer subjected to adverse and favorable pressure gradients was conducted at Mach number 4 for a free-stream Reynolds number of 0.50×10^6 per inch. Two severe pressure gradients were imposed on the boundary layer by interchangeable, contoured centerbodies inside a large hollow cylinder for cold-wall and adiabatic-wall temperature conditions. Imposition of either of the adverse pressure gradients significantly decreased the natural growth rate of the boundary-layer displacement thickness, whereas the favorable pressure gradient had opposite effects; momentum thickness was relatively unaffected by pressure gradient. A pressure gradient increase of about 30 percent caused relatively small changes in the skin friction, heat-transfer rate, and the characteristic boundary-layer parameters. Wall cooling effects ($T_w/T_O \approx 0.3$) on the boundary-layer thickness parameters were nearly insignificant, in comparison with the adiabatic-wall results. Heat-transfer distributions were similar to the local skin friction results based on free-stream conditions.

Each transmittal of this document outside the Department of Defense must have prior approval of SAMSO/TRD-STINFO, AF Unit Post Office, Los Angeles, California 90045.

DD FORM 1473

14. KEY WORDS	LINK A		LINK B		LINK C	
	ROLE	WT	ROLE	WT	ROLE	WT
turbulent boundary layer						
pressure gradients						
heat transfer						
supersonic flow						
cylindrical bodies						

1 Turbulent boundary layer —